Since January 2020 Elsevier has created a COVID-19 resource centre with free information in English and Mandarin on the novel coronavirus COVID-19. The COVID-19 resource centre is hosted on Elsevier Connect, the company's public news and information website.

Electron Microsc. Rev., Vol. 3, pp. 1–27, 1990.
Printed in Great Britain.

0892-0354/90 $0.00 + 0.50

VIROLOGICAL APPLICATIONS OF THE GRID-CELL-CULTURE TECHNIQUE

ALEX D. HYATT and BRYAN T. EATON

Commonwealth Scientific and Industrial Research Organisation, Australian Animal Health Laboratory, P.O. Bag 24, Geelong, Victoria, 3220, Australia

Abstract—Whole mounts of intact virus-infected cells have been used for several decades to examine virus–cell relationships and virus structure. The general concept of studying virus structure in association with the host cell has recently been expanded to reveal interactions between viruses and the cytoskeleton. The procedure permits utilization of immuno-gold protocols using both the transmission and scanning electron microscopes. The grid-cell-culture technique is reviewed to explain how it can be exploited to provide valuable information about virus structure and replication in both diagnostic and research laboratories. The use of the technique at the research level is discussed using bluetongue virus as a model. The procedure can provide basic structural information about intact virions and additional data on the intracellular location of viruses and virus-specific structures and about the mode of virus release from infected cells. Application of immunoelectron microscopy reveals information on the protein composition of not only released virus particles but also cell surface and cytoskeletal-associated viruses and virus-specific structures. Collectively, this simple and physically gentle technique has provided information which would otherwise be difficult to obtain.

CONTENTS

I. Introduction 1
II. Culturing cells on electron microscope grids 2
A. Virus infection of cells 3
III. Examination of unextracted virus-infected cells 3
A. Application to diagnosis 4
B. Enveloped viruses 4
C. Non-enveloped viruses 9
IV. Examination of extracted virus-infected cells 11
V. Application of immuno-gold-electron microscopy 13
A. Transmission electron microscopy 13
B. Scanning electron microscopy 17
VI. Virus structure and morphogenesis: Bluetongue virus 20
A. Virus structure 20
B. Intracellular and extracellular virus 20
C. Location and composition of virus specific structures 23
D. Mode of virus release 24
VII. Concluding remarks 25
Acknowledgements 25
References 25

1. INTRODUCTION

Unsectioned tissue culture cells have been used in electron microscopical studies since the 1940s. These cells or whole mounts, as they were referred to, provided the vehicle for the examination of cell ultrastructure and virus–cell interactions. Today ultramicrotomy has largely replaced this early embedment-free technique as the primary procedure for investigating cellular ultrastructure and virus

morphogenesis. The current popular choice for ultrastructural analyses of purified virus is negative contrast electron microscopy (NCEM) (Brenner and Horne, 1959). Other techniques which are less commonly used include cryo-electron microscopy of vitrified layers of virus suspensions (Adrian *et al.*, 1984; Dubochet *et al.*, 1985; Vogel *et al.*, 1986; Hosaka and Watabe, 1988) and freeze fracturing (-etching) of virus suspensions and infected cells (Bauer and Medzon, 1971; Nermut, 1973, 1978; Darcy-Tripier *et al.*, 1984).

There has been a recent revival in the use of whole mounts particularly in the examination of the cytoskeleton of uninfected and infected cells (Brown *et al.*, 1976; Lenk *et al.*, 1977; Lenk and Penman, 1979; Bohn *et al.*, 1986; Hyatt *et al.*, 1987; Eaton *et al.*, 1987, 1988). The relevance of whole mounts for viral studies are obvious. The examination of whole cells provides the opportunity to visualize, at high resolution, large proportions of cytoplasmic volume with minimum disruption to the cells. This can reveal various stages of virus replication within infected cells such as adsorption, penetration, uncoating, morphogenic steps in virus assembly and release of completed viruses from the infected cells.

The potential therefore exists to study the three-dimensional relationship between animal viruses, their replicative intermediates and cellular constituents. This is not always possible with the use of ultra-thin plastic sections as there is frequently a masking of non-membrane-bounded protein structures by the embedding resin (Penman, 1985). Using whole mounts it is comparatively easy to map the distribution of receptor sites on cell surfaces and to study the adsorption of virions to the receptors and any resultant morphological alterations of the virion and cell. The mode of virus penetration (that is, translocation, endocytosis or fusion of the virus envelope with the plasma membrane) can be observed without the need for ultramicrotomy, as can also the maturation and release of the progeny virions. The technique also facilitates virus morphological studies as the progeny virions adsorbed to the grid substrate outside the cell are extremely well preserved (De Harven *et al.*, 1973; Hyatt *et al.*, 1987). The absence of any severe physical or biochemical treatment in the overall culturing and infection of cells results in the generation of little to no artifactual virus structures and thus provides an excellent procedure for virus diagnosis and taxonomic studies.

The success of whole mounts in virology are due to the numerous post-culturing procedures which can be used to facilitate any of the above investigations. This was shown by Hyatt *et al.* (1987) when virus-infected grid-cell-cultures were either negatively stained, extracted with non-ionic detergents, critical point dried and/or used for immunoelectron microscopy (IEM). Examination of one or more of the preparations collectively, provided valuable information for virus diagnosis (Hyatt *et al.*, 1987), expression of neutralization epitopes (Gould *et al.*, 1988; Hyatt *et al.*, 1988); virus morphogenesis (Eaton *et al.*, 1987, 1988) and location of intracellular virus specific proteins (Eaton *et al.*, 1988; Hyatt and Eaton, 1988). In this review the application of whole mounts, in particular the grid-cell-culture technique (Hyatt *et al.*, 1987) to various fields of virology such as virus diagnosis and virus morphogenesis are discussed.

II. CULTURING CELLS ON ELECTRON MICROSCOPE GRIDS

Whole cells destined for examination by transmission electron microscopy (TEM) are generally prepared by one of two procedures. The first involves cultivation of cells on filmed (for example formvar-carbon) sterile glass or plastic substrates (Buckley and Porter, 1967, 1975; Buckley and Raju, 1976; Bohn *et al.*, 1986). The other method involves cultivation of cells on electron-lucent filmed, acid-washed gold electron microscope grids (Brown *et al.*, 1976; Bell, 1981; Borrelli *et al.*, 1985; Ornelles *et al.*, 1986; Hyatt *et al.*, 1987). The filmed grids are usually stabilized with carbon and sterilized in 70% ethanol or by UV irradiation (Borrelli *et al.*, 1985; Hyatt *et al.*, 1987). We have found this method more efficient than the sandwich practice (placement of grids between film and coverslip) because there were no difficulties with lifting of films or the removal and processing of individual grids. Cells were easily cultivated on either form of substrate by transfer to tissue culture dishes and

addition of a cell suspension in the appropriate medium. The cells are allowed to settle and spread for 24 hr before use. However, occasional difficulties with cell attachment and growth can be encountered. Such difficulties can be mainly attributed to the hydrophobic nature of the filmed substrate and can be rectified by glow discharging the filmed substrates (in air) or washing them with detergent such as 0.1% triton X-100 or 0.1% NP40 for several minutes prior to overnight incubation in tissue culture medium in the absence of cells.

The degree of cell confluency is also important, particularly for some subsequent preparative procedures. If, for example, the cell cultures are critical point dried, then high cell confluency has minimal effect except that little or no areas of substrate are available for released viruses to adsorb and this clearly limits the possibility of examining extracellular and surface cell-associated viruses. Alternatively, if the cells are to be negatively stained and air dried then the presence of too many cells will result in splitting and destruction of the supportive film due to severe shrinkage of large numbers of cells. This problem can be rectified by reducing the number of cells and/or the application of slightly thicker films.

A. *Virus Infection of Cells*

Cells are infected by adding a virus solution to the tissue culture dishes containing the filmed substrates. Alternatively if the virus stock solution is limited, each grid can be incubated in 20–50 μl droplets of virus suspension. The dilution of the virus suspension depends upon the desired multiplicity of infection and, when virus diagnosis is involved, the nature of the clinical sample (where cell toxicity may be a problem). Tissue culture dishes are placed at 37°C for 1 hr to permit virus adsorption following which the solution is replaced with fresh tissue culture growth or maintenance media.

III. EXAMINATION OF UNEXTRACTED VIRUS-INFECTED CELLS

The major disadvantage of using whole mounts in TEM is the inability of the electron beam to penetrate the specimen. The use of critical point drying (De Harven *et al.*, 1973; Buckley and Porter, 1975) and high voltage electron microscopy (HVEM) techniques (Kilarski *et al.*, 1976) have provided a partial solution to this problem.

One of the earliest uses of critical point drying, in the study of animal viruses, involved purified oncornaviruses (De Harven *et al.*, 1973). The success in visualizing viruses adsorbed to the grid was attributed to a combination of positive staining with uranyl acetate and critical point drying. The viruses were easily identified and resembled those in thin sections. Variations of this approach followed, including those of Malech and Wivel (1976) who critical point dried purified murine intracisternal A particles which had been adsorbed to filmed grids and shadowed them with platinum–iridium. Replicas of critical point dried and freeze dried cells have also been used to analyze the interaction of vesicular stomatitis virus (Birdwell and Strauss, 1974) and murine mammary tumour virus (Sheffield, 1981) with cells. Overall, these procedures have revealed cell-associated and budding viruses which have provided valuable information on virus morphology and topography of cell surface-associated viruses during morphogenesis.

Critical point drying and examination of whole cells at 100 kV can reveal the three-dimensional structure of cultured cells (Kilarski and Koprowski, 1976). The lack of embedding media facilitates these observations and enables many intracellular and extracellular virus–cell interactions to be studied. The advantanges of this technique in virological studies were noted by Iwaski (1978) and include (a) rapid screening of both intracellular and extracellular aspects of numerous virus-infected cells and (b) *in situ* fixation of both released virions and those in the process of being released from host cells. The noted disadvantages of this technically simple procedure included the uncertainty about the identity of some intracellular structures and poor visibility of structures within the vicinity of the nucleus due to the thick central nuclear region.

HVEM has also been used to visualize viruses such as vaccinia, parainfluenza, herpes simplex type 1 and frog virus 3 within whole infected cells (Grimly, 1970; Kilarski *et al.*, 1976; Stokes,

1976a,b; Murti *et al.*, 1984; Yoshida *et al.*, 1986). The use of this technique however is limited by access to the specialized equipment.

NCEM has also been used to examine whole cells infected with rabies, mouse mammary tumour, influenza and bluetongue viruses (Dales, 1962; Choppin, 1963, Kramarsky *et al.*, 1970; Iwasaki, 1978; Hyatt *et al.*, 1978). In the early studies virus-infected cells were either cultured in suspension or on glass substrates. Infected cells grown on substrates were trypsinized prior to further handling. The cells were, in the majority of studies, swollen using hypotonic saline, fixed, pelleted, washed, resuspended and then adsorbed to formvar-carbon coated grids prior to staining with 2% sodium phosphotungstate. The information obtained from examination of these preparations must be considered with caution as deleterious effects on virus structure and virus cell interactions may be consequential to either osmotic shock or enzymatic treatment of the cells. Iwasaki (1978) cultured cells on formvar-carbon copper grids which had been placed on plastic cover slips. Although the copper grids were theoretically removed from direct contact with the cells and medium the procedure has the potential for causing a cell toxicity problem. Despite this, Iwasaki (1978) was successful in cultivating virus-infected cells and examining them by both critical point drying and NCEM. Hyatt *et al.* (1987) seeded cells on to biologically inert carbon parlodion filmed gold grids. The cells were infected by adding virus suspension to tissue culture filled petri dishes containing the grids. Upon first indications of a cytopathic effect the grid-cell-cultures (GCC) were fixed in 2.5% glutaraldehyde, washed in isoosmotic buffer, post fixed in osmium tetroxide, washed in distilled water and stained with 2% potassium phosphotungstate. These preparations were used, as described below, to examine various viruses and virus cell interactions.

Nermut (1982) cautions against stringent interpretations of negatively stained preparations because, for example, enveloped viruses can collapse and distort due to the severe surface tensions generated by air drying. Such artifacts can be manifested in the form of particle pleomorphism and "tails". However, if the preparations were fixed prior to air drying the images were more likely to represent *in situ* structures and thus "reasonable information can be obtained" (Nermut, 1982). Air drying of negatively stained GCC has been used in our laboratory to identify progeny viruses amplified in GCC, the parental viruses of which were submitted to the laboratory in the form of diagnostic clinical samples.

A. *Application to Diagnosis*

Electron microscopy still has a significant role in viral diagnosis. Traditionally NCEM has been used to visualize viruses from clinical and passaged biological material. Occasionally viruses cannot be visualized in clinical material due to the inherent low number of virions (even after concentration) or a confident identification cannot be made because of the presence of virus-like artifacts. Furthermore the virus structures may have been inadvertantly altered due to ultracentrifugation through density gradient columns such as sucrose or caesium chloride (Hyatt *et al.*, 1987). Under such circumstances it would be necessary to amplify the virus in tissue culture and/or use a technique which minimized the generation of artifactual material and adverse physical forces. The use of GCC provides the means for satisfying these objectives. Fixation of GCC results in the *in situ* preservation of progeny viruses on the grid substrate and in association with the cell. The viruses can be easily observed, contrasted against an artifact-free background and ideally presented for IEM. The application and success of the technique in virus diagnosis is discussed below.

B. *Enveloped Viruses*

When appropriate host cells are infected with virus, the progeny viral particles can be observed in association with both the grid film substrate and the cell. Representatives of the families Togaviridae, Orthomyxoviridae, Paramyxoviridae, Rhabdoviridae, Poxviridae, Coronaviridae, Bunyaviridae, Herpesviridae and Iridoviridae have so far been identified using the grid-cell-culture technique in our laboratory. Valuable information about virus shape, dimensions and mechanism of

release (and thus derivation of envelope) are easily obtained with the technique. The viruses discussed below are examples of how the accumulation of such data can facilitate viral diagnosis. The application of the technique to the collection of information on virus morphogenesis is discussed in Section VI.

When cells were infected with Newcastle disease virus (NDV, paramyxovirus) virions could be observed budding from the host cell plasma membrane. The particles are either spherical or filamentous (Fig. 1) whereas those adsorbed to the grid substrate take on a more spherical appearance. Nucleocapsids (Figs 1B and 13C) can occasionally be visualized in both forms of the virus or lying free on the substrate. The infected cells may also exhibit modified thickened areas of plasma membrane, which may represent areas of M protein accumulation (Nagai *et al.*, 1983). From these thickened areas "rigid", irregular protusions are frequently observed (Fig. 1B). The presence of these structures can be confirmed by examination of ultra-thin sections of similarly infected cells. Surface projections in many of these negatively stained viruses can be difficult to observe. It is believed that prefixation with glutaraldehyde or osmium tetroxide can produce a disorganizing effect on similar projections in other viruses (Nermut, 1972; von Bonsdorff and Harrison, 1975; Nermut, 1982). We have found that this problem is more pronounced when viruses (fixed *in situ*) were in the process of budding. Examination of cells infected with avian influenza virus (AIV, Orthomyxoviridae) do not exhibit peripheral areas of membrane thickening and the budding virions generally approximate a filamentous shape (of uniform width) from which virions appear to "pinch" (Fig. 2). These (NDV and AIV) are examples of viruses which derive their envelope from the plasma membrane. The *in situ* fixation minimizes the pleomorphic appearance of viruses and thus further enables virus identification based on virus morphology.

Alphaviruses and flaviviruses are reported to be morphologically similar (Palmer and Martin, 1982). They are spherical (40–70 nm) with alphaviruses

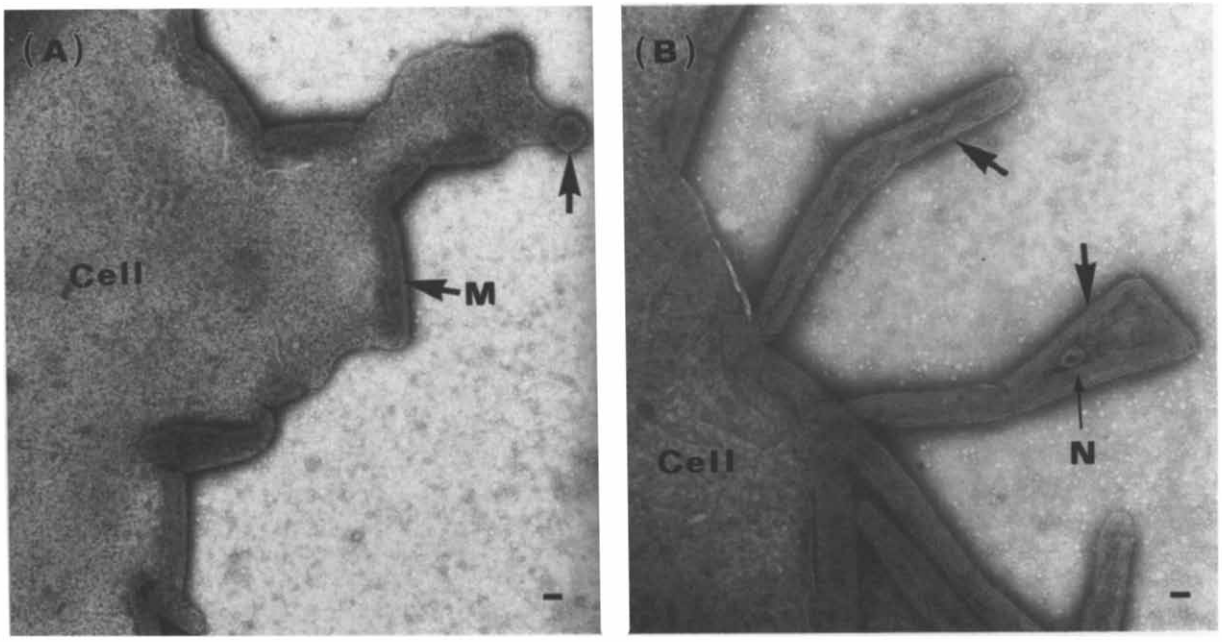

Fig. 1. Negative stained air dried whole cells infected with a paramyxovirus (Newcastle disease virus, NDV). (A) spherical form of virus (arrow) budding from the surface membrane. Thickened areas of membrane, presumably representing accumulation of "M" membrane (M), are apparent. (B) Filamentous forms of NDV budding from the cell surface (arrows). Nucleocapsids (N); cell (C). Scales represent 100 nm.

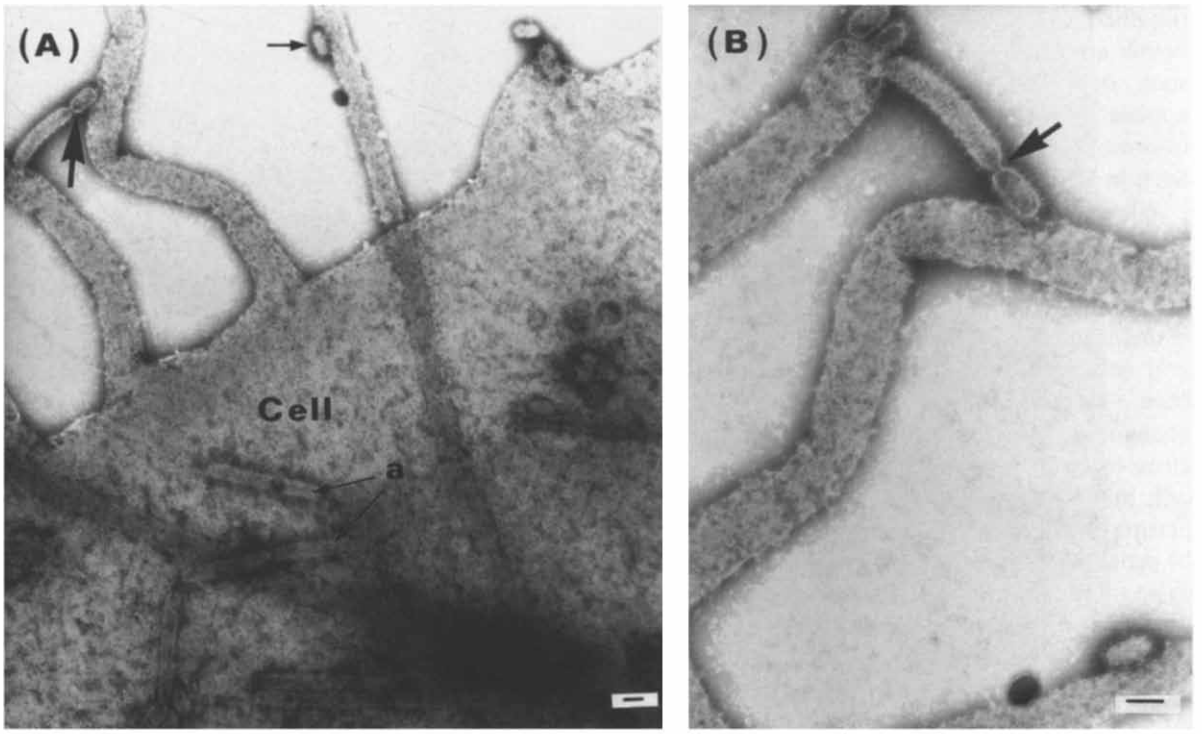

Fig. 2. Negative stained air dried whole cells infected with an orthomyxovirus (avian influenza virus, AIV). (A) Filamentous forms of AIV budding from the apical (a) and lateral (arrows) surface membranes. A filamentous form is indicated (large arrow) from which a virus is "pinching". (B) Enlargement of "pinching" AIV, the surface associated protrusions are indicated (arrow). Scales represent 100 nm.

being the larger. Flaviviruses although accepted to be smaller have been reported in the size range of 40–60 nm (Murphy, 1980). They are also reported to have 7 nm rings on the virion surface and possess an intracellular-derived envelope, whereas purified alphaviruses have a conspicuous $T = 4$ icosahedral structure and derive their envelope from the plasma membrane. If problems arise in the identification of viruses within this size group (40–70 nm), then examination of virus particles by GCC can reveal details of the virion surface structure and the derivation of the associated envelope (intracellular or plasma membrane). Figures 3A and B illustrate the above with alphavirus-infected cells (Ross River virus). The virus can be observed budding from the plasma membrane and the demarcating surface subunits are apparent.

Akabane virus (Bunyaviridae), like other members of the group, is a difficult virus to visualize as it is known to be very fragile and sensitive to physico-chemical treatment (Munz *et al.*, 1981). Bunyaviruses derive their associated membranes by budding into intracytoplasmic cisternae (Murphy *et al.*, 1973). Examination of Akabane virus-infected GCC reveal abundant, intact membraneous viruses against a clean background (Fig. 3C). The viruses can also be observed in association with the plasma membrane (Fig. 3D). The structure of these did not differ significantly from that of released or adsorbed particles. Extensive examination of the infected cells did not reveal budding viruses (that is, viruses acquiring a membrane from the plasma membrane) however, viruses with associated envelopes could be observed crossing the cell membrane. Other membrane associated viruses, but with well defined shape, which have been detected with this technique are shown in Figs 4 and 5.

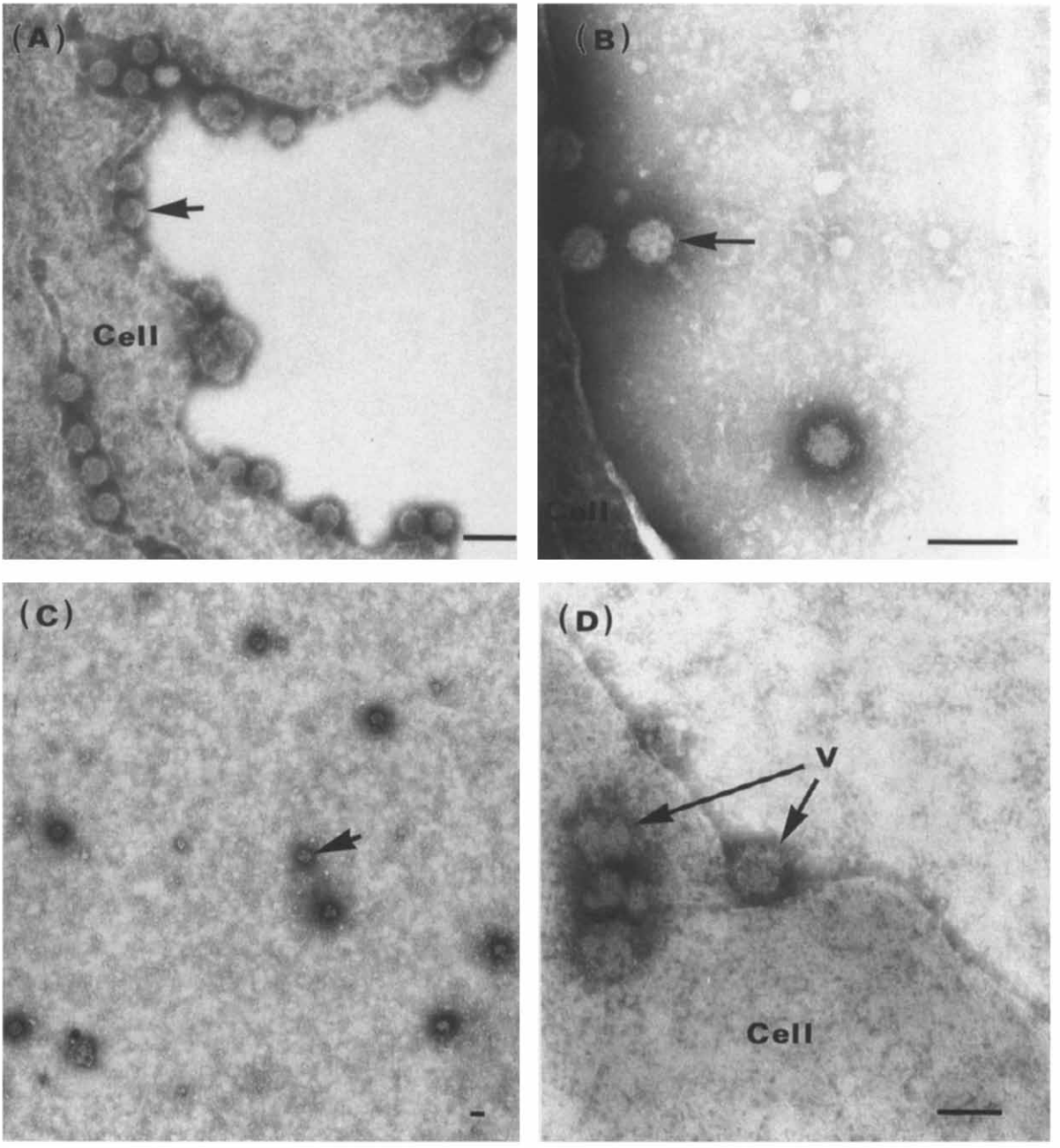

Fig. 3. Negative stained, air dried whole cells infected with an alphavirus (Ross River) and a bunyavirus (Akabane). (A) Ross River virus budding from the surface membrane (arrow). (B) Higher magnification illustrating the surface subunits and projections associated with Ross River virus (arrow). (C) Akabane virus (arrow) in association with the grid substrate. (D) Akabane virus (V) associated with the cell surface. Scales represent 100 nm.

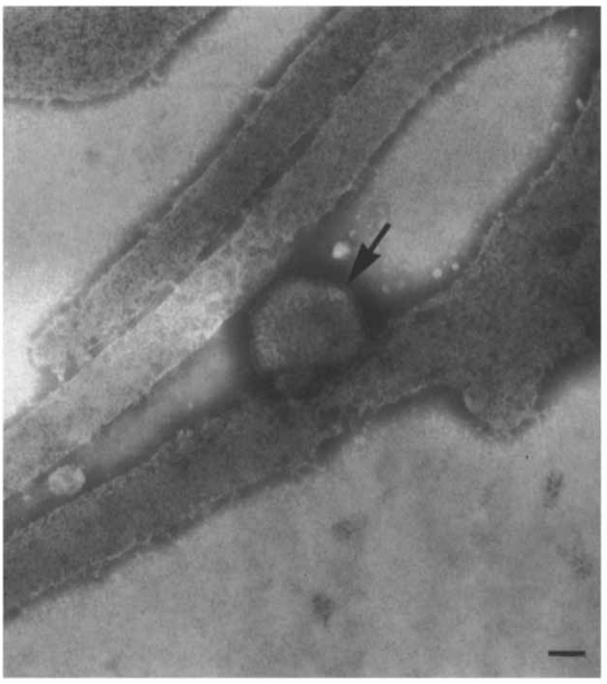

Fig. 4. Negative stained, air dried whole cell infected with a poxvirus. Vaccinia virus (arrow) is shown 18 hr post-infection associated with a cellular process. Scale represents 100 nm.

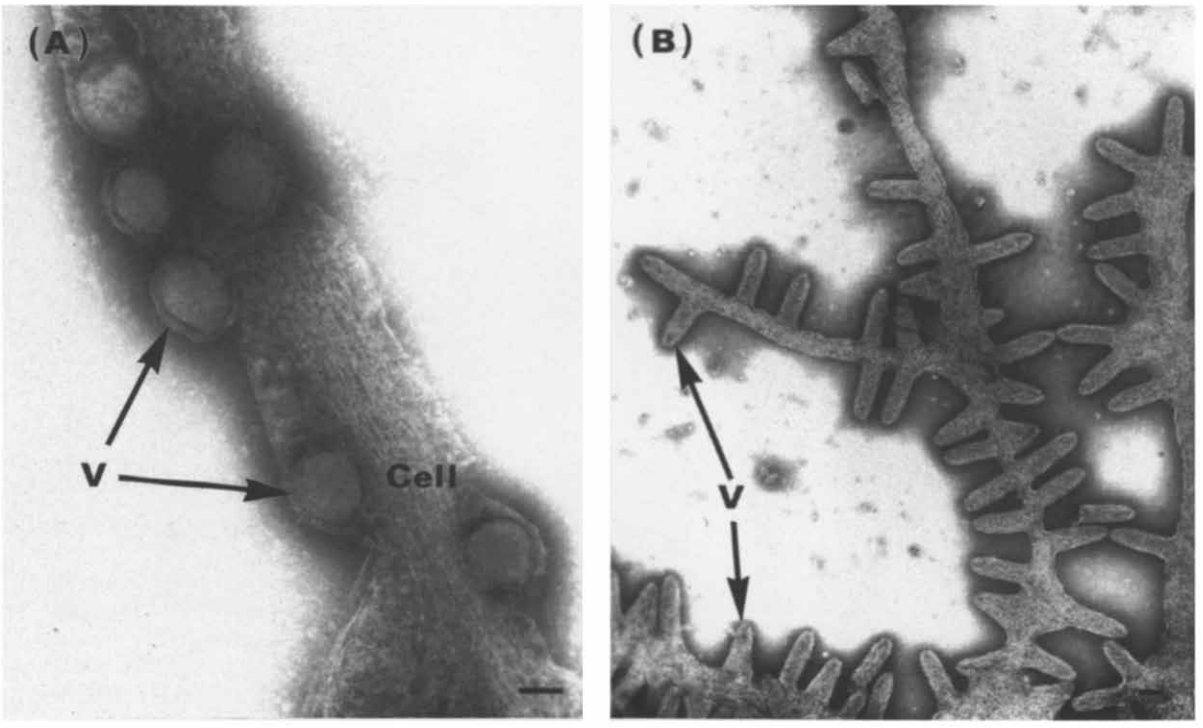

Fig. 5. Negative stained, air dried cells infected with (A) an iridovirus, (epizootic haematopoietic necrosis virus), and (B) rhabdovirus (bovine ephemeral fever virus). Viruses (v). Scales represent 100 nm. (Adapted from Hyatt *et al.*, 1987.)

B. *Non-enveloped Viruses*

Non-enveloped viruses can also be visualized with GCC. Representatives of Reoviridae, Adenoviridae, Parvoviridae and Birnaviridae have been identified in this laboratory using this technique. Representative viruses from some of these families are discussed below.

Bluetongue virus (BTV), which is a member of the orbivirus genus in the family Reoviridae, is a 60–70 nm icosahedral virus with a fibrillar outer coat (Hyatt *et al.*, 1987; Hyatt and Eaton, 1988). When crude preparations are used for NCEM the intact virion may be difficult to identify amongst the background material. Alternatively when the viruses are subjected to laboratory manipulation (for example, ultracentrifugation through density gradients) the outer coat often is partially or totally removed to reveal a capsid with large ring-shaped capsomeres (Fig. 6A). Therefore the morphology of orbiviruses may be altered by the preparative techniques used. Diagnosticians should be aware of these variations or alternatively use a less disruptive technique such as the grid-cell-culture technique.

Analysis of BTV-infected GCC revealed numerous virions adsorbed to the grid substrate, underlying the cell surface and being released from the cell. The virus surface was not disrupted and exhibited a fine fibrillar outer coat (Fig. 7A). Similar virions were observed intracellularly (Fig. 7B) and were occasionally associated with cellular filaments. Virions were also observed exiting the cell by extrusion and budding from the surface membrane (Figs 7C, D). Collectively the data provided valuable information for virus diagnosis (virus size, surface topography, association with cellular components and the modes of virus release).

The sensitivity of the grid-cell-culture technique for other non-enveloped viruses such as birnaviruses, adenoviruses and adeno-associated viruses (AAV) is shown in Fig. 8. The small 18–28 nm icosahedral AAV were obvious against a clean background which indicated the suitability of the technique for the detection of parvoviruses. Adenoviruses could also be observed on the grid substrate and entering host cells; Fig. 8B shows a particle entering a cell presumably by endocytosis. Birnaviruses and adenoviruses were also examples of lytic viruses, that is viruses which gain release

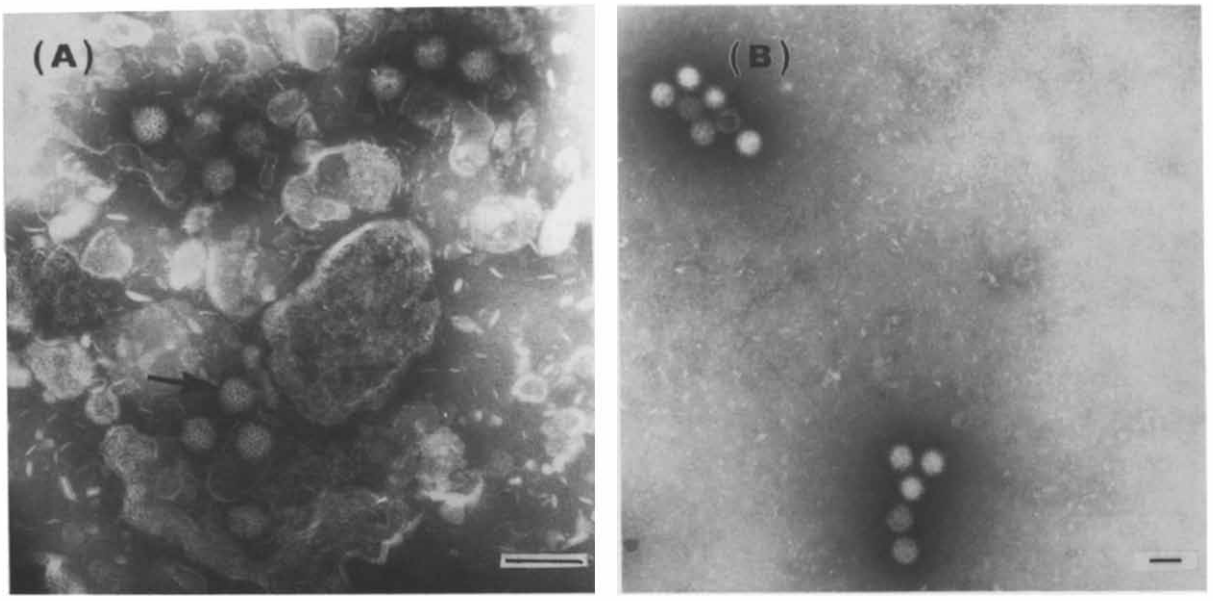

Fig. 6. (A) Negatively stained bluetongue virus after ultracentrifugation. The outer coat has been removed and the capsomeric cores (arrow) can be observed amongst cellular debris. (B) Bluetongue virus prepared by the grid-cell-culture technique. The outer coat is intact. Scales represent 100 nm.

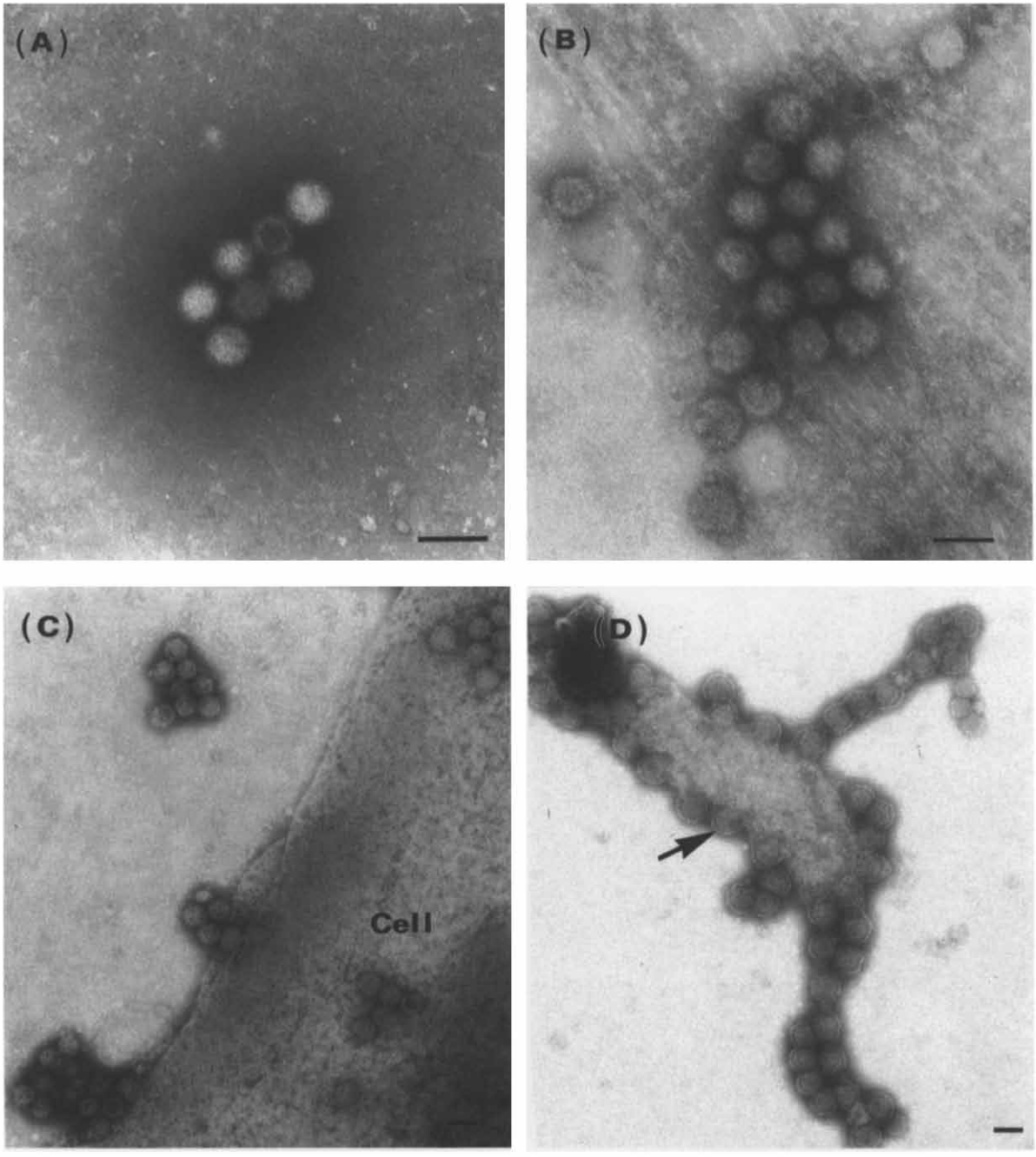

Fig. 7. Negative stained, air dried whole cell infected with an orbivirus (bluetongue virus, BTV). (A) Viruses adsorbed to grid substrate. Note the fribrillar outer coat. (B) BTV underlying the cell surface. (C) BTV aggregates, 18 hr post-infection, extruded from an infected cell. (D) BTV budding from the plasma membrane (arrow). Scales represent 100 nm. (Adapted from Hyatt *et al.*, 1987.)

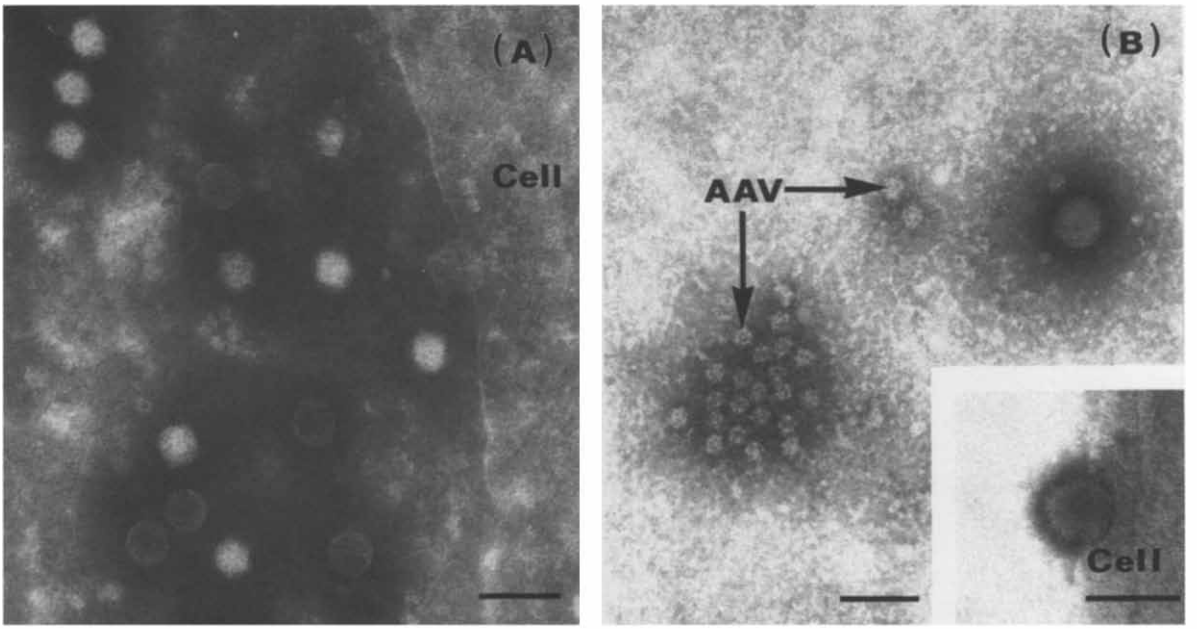

Fig. 8. Negative stained, air dried whole cells infected with (A) biravirus (infectious pancreatic necrosis virus) and (B) adenovirus (P11537/82); note the presence of adeno-associated virus (AAV). Inset, adenovirus entering a host cell, presumably by endocytosis. Scales represent 100 nm.

from host cells following cell lysis. It is possible to locate these particles and associated structures on the grid substrate (Fig. 8). When lytic viruses are being used it may be necessary to leave the harvesting of GCC until advanced CPE has occurred as this would optimize the chance of virus detection but have the disadvantage of producing a comparatively high background (Fig. 8A). This disadvantage was not severe if the viruses involved are icosahedral non-enveloped particles.

IV. EXAMINATION OF EXTRACTED VIRUS INFECTED CELLS

Biological functions often ascribed to the cytoskeleton of eukaryotic cells include cell movement, adhesion, division, organization of organelles and molecules and virus metabolism (Ben-Ze'ev *et al.*, 1981; Penman, 1985; Bell *et al.*, 1988). The cytoskeleton is generally defined as a three-dimensional network of microtubules, intermediate filaments and microfilaments consisting of specific core proteins and filament-specific associated proteins (Bell *et al.*, 1988). One of the above functions, virus metabolism, can be exploited from a diagnostic viewpoint as many viruses and/or virus-specific proteins are associated with some aspect of the cytoskeleton during their replicative cycle. The viruses include poliovirus (Lenk and Penman, 1979), measles virus (Bohn *et al.*, 1986), vesicular stomatitis virus (Cervera *et al.*, 1981) and representatives from the following families: Papoviridae (Ben-Ze'ev *et al.*, 1982), Iridoviridae (Murti *et al.*, 1985), Poxviridae (Hiller *et al.*, 1979), Herpesviridae (Ben-Ze'ev *et al.*, 1983), Adenoviridae (Luftig and Weihing, 1975) and Reoviridae (Eaton *et al.*, 1987).

Many methods have been used to observe the cytoskeleton. These include TEM of ultra-thin sections, whole and detergent-extracted cells and platinum–carbon replicas of frozen and fractured cells, NCEM and scanning electron microscopy (SEM) of detergent extracted cells and HVEM of whole and extracted cells (Bell *et al.*, 1988). With the grid-cell-culture technique satisfactory cytoskeletons can be prepared by washing the GCC with a mixture of 1% triton X-100 or 1% NP40 in

0.1% glutaraldehyde (in buffer of choice) for 2 min and critical point drying from carbon dioxide (Hyatt *et al.*, 1987). The preparations remain attached to the filmed-grid substrate and can be coated or viewed directly at 50 kV in a transmission electron microscope (Fig. 9). The preparation of cytoskeletons including conditions required for minimizing depolymerization and extraction of cytoskeletal proteins are described by Small (1988).

A common problem with whole mount cytoskeletons is that interpretation of conventional two-dimensional photographic images can often be difficult as they represent a three-dimensional network of interconnecting filaments. The use of stereopairs can help avoid the problem by revealing the spatial organization of and viral association with the cytoskelton. Cytoskeletons prepared and recorded in the above manner can prove beneficial in diagnostic virology and virus morphogenesis studies. The main advantages are (a) conventional thin sections, which provide comparatively poor detail on cytoskeletal organization and take the major part of a working day to prepare, are not required for the identification of intracellular viruses and related structures; (b) preparation time is less than 90 min and (c) the inter-relationship between virus and cell can be studied in a three-dimensional matrix which facilitates in identification and localization of structural components of the cytoskeleton and any associated viral components.

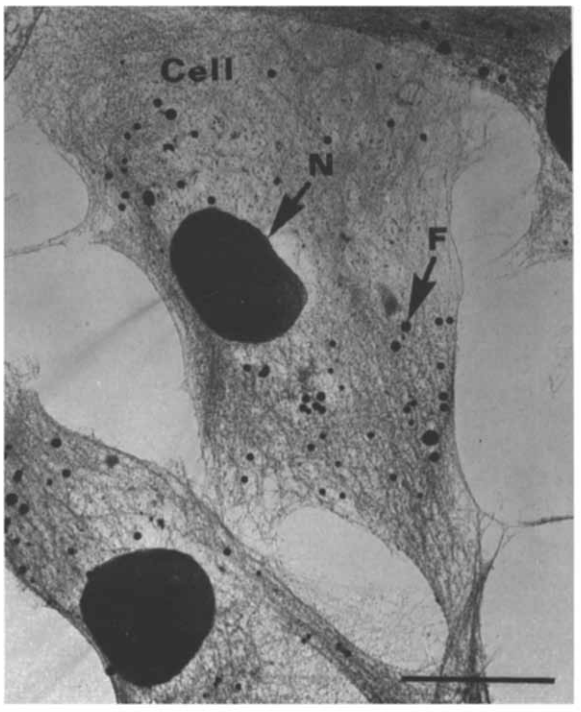

Fig. 9. An extracted uninfected, tissue culture cell critical point dried from carbon dioxide, carbon coated and examined at 50 kV. Nucleus (N), fat droplets (F). Scale represents 10 nm. (Adapted from Eaton *et al.*, 1987.)

Figures 10 and 11 illustrate the usefulness of the grid-cell-culture technique for the intracellular localization of poxviruses (vaccinia), iridoviruses (epizootic haematopoetic necrosis virus, EHNV) and orbiviruses (BTV) and their associated structures. The successful use of the technique in diagnostic virology depends upon the knowledge of the diagnostician. For example, orbivirus-infected cells are known to contain viruses, virus inclusion bodies and virus-specified tubules all of which are associated with the cytoskeleton (Eaton *et al.*, 1987), thus examination of cytoskeletons will reveal these characteristic orbivirus-specific structures. Diagnosticians must also be familiar with the appearance of unstained virus particles and be capable of discriminating cellular from viral structures. This is not a problem for larger viruses such as EHNV, BTV and vaccinia which are shown in Figs 10 and 11.

The extraction technique described above generates an open cytoskeletal framework containing the majority of the cells polyribosomes and a dense nuclear matrix. Ben-Ze'ev *et al.* (1983) and Penman (1985) described the use of DNAase, RNAase and $(HN_4)SO_4$ to extract the chromatin fraction from nuclei to produce a semi-translucent nuclear matrix–intermediate filament scaffold. Ben-Ze'ev *et al.* (1983) used this approach to visualize herpes simplex virus (Herpesviridae) bound to the nuclear matrix of an infected cell. It should also be possible to visualize small cytoskeletal-associated viruses or virus-associated structures by treating cells with puromycin prior to generation of the cytoskeleton. This drug disrupts polyribosomes and thus should strip the cytoskeleton of similarly-sized cellular structures. Alternatively, when small viruses or enveloped viruses with nondescript nucleocapsids

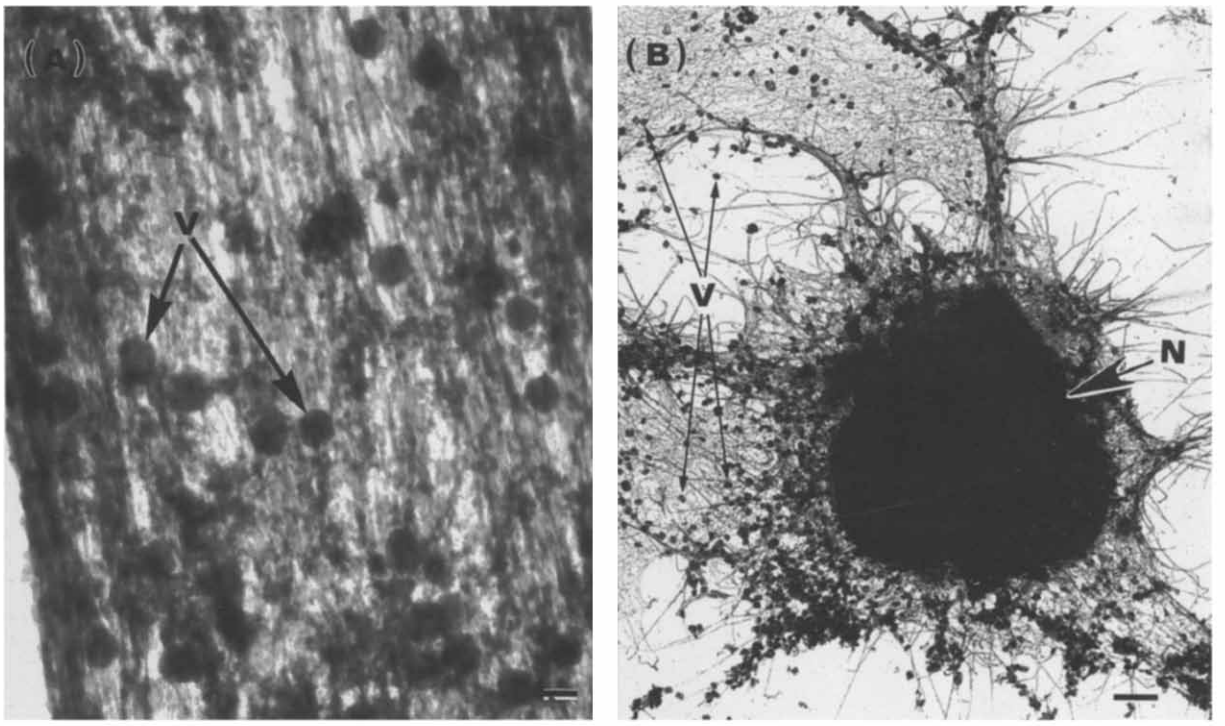

Fig. 10. Whole tissue culture cells, extracted 18 hr post-infection and critical point dried from carbon dioxide. (A) Iridovirus (epizootic haematopoietic necrosis virus). Scale represents 100 nm. (B) poxvirus (vaccinia). viruses (V), nucleus (N). Scale represent 1 μm.

are involved, IEM (Section V) may be used for their identification.

It should be noted that cytoskeletons can also provide valuable information on the location of viruses, that is whether they are found predominantly in the soluble or insoluble phase of the cell. Orbiviruses, for example, are associated with the cytoskeleton (insoluble phase) of infected cells and thus any procedures involving purification of these viruses may incorporate a step which shears the particles from the cytoskeletal filaments.

V. APPLICATION OF IMMUNO-GOLD ELECTRON MICROSCOPY

A. Transmission Electron Microscopy

Both unextracted and extracted GCC can be used for IEM. Currently, colloidal gold probes are being successfully used for microbiological immunocytochemistry (Beesley, 1988; Carrascosa, 1988). These probes are generally complexed to protein A, protein G, monospecific or polyspecific antibodies and streptavidin. In practice they are used directly or indirectly for the detection of specific antigens by a range of methodologies including post-embedding, pre-embedding, immuno-negative stain and immuno-replica techniques. GCC can be used as alternatives to the classical immuno-negative stain and plastic embedding techniques.

Figure 12 illustrates the use of the technique in the gold labelling of unextracted BTV-infected cells. Gold-labelled viruses can be observed on the filmed grid substrate and on the surface of the infected host cell. Labelling was achieved by the use of gold-complexed monoclonal antibody (Mab) to a virus outer coat protein, VP2. Although the preparation had been pretreated with 0.1% glutaraldehyde (to maintain cell structure and prevent removal of cells from the grid during washing

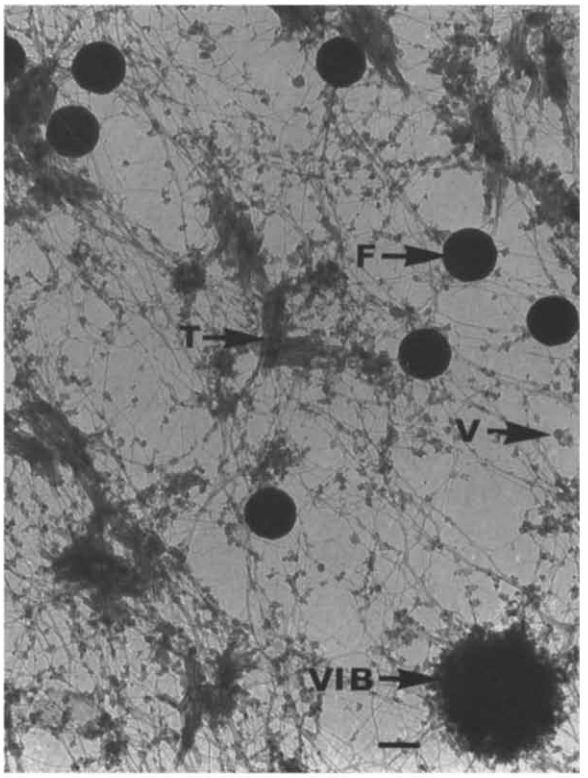

Fig. 11. Whole tissue culture cells, extracted 18 hr post-infection with bluetongue virus and critical point dried from carbon dioxide. Virus inclusion body (VIB), virus tubules (T), virus (V), fat droplet (F). Scale represents 200 nm. (Adapted from Eaton *et al.*, 1987.)

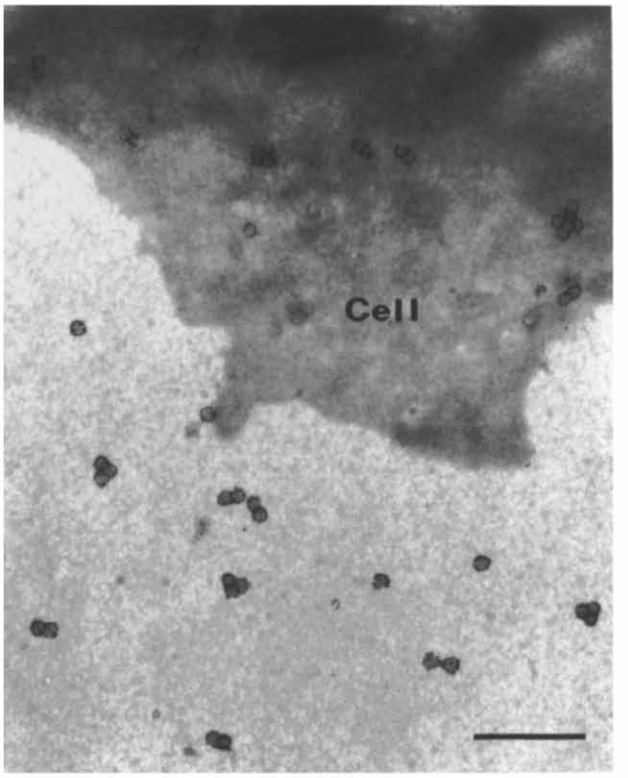

Fig. 12. Bluetongue virus infected cells probed with a monoclonal antibody complexed with 12 nm colloidal gold. Scale represents 1 μm. (Adapted from Hyatt and Eaton, 1988.)

procedures) no detrimental effects due to (a) free aldehyde groups (manifested as non-specific labelling) or (b) poor labelling due to possible adverse effect on the reactivity of the Mab to specific aldehyde-fixed antigenic sites, were apparent. The micrograph indicates that the labelling is specific and intense. Similar results were routinely obtained in this laboratory for a range of viruses including herpesviruses, alphaviruses, coronaviruses, paramyxoviruses and bunyviruses; some of these are illustrated in Fig. 13. The labelling depicted in the electron micrographs cover direct and indirect procedures utilizing gold-labelled monoclonal antibodies and gold-complexed protein A. The success of this technique can be attributed to its simplicity and its overall non-destructive nature which maintains surface-associated antigens. Details of the methodology are given in Hyatt *et al.* (1987).

IEM can also be performed on extracted cells. The technique is rapid (2–4 hr) but has the limitation that only the insoluble fraction of a cell has the potential to be labelled. Despite this limitation the concept has been used by Bohn *et al.* (1986) to study the involvement of actin filaments in the budding of measles virus and Eaton *et al.* (1987, 1988) to study the association and protein composition of BTV-specific structures attached to the cytoskelton. A major benefit of using extracted GCC for IEM is the ability of antibodies and gold probes to freely diffuse through the cytoskeletal matrix and interact with the intact virus structures. Thus antibody–antigen interactions will be optimized in a biological system where normally, with post-embedding techniques, the antigenic mass of the viruses or associated structures is so low that few

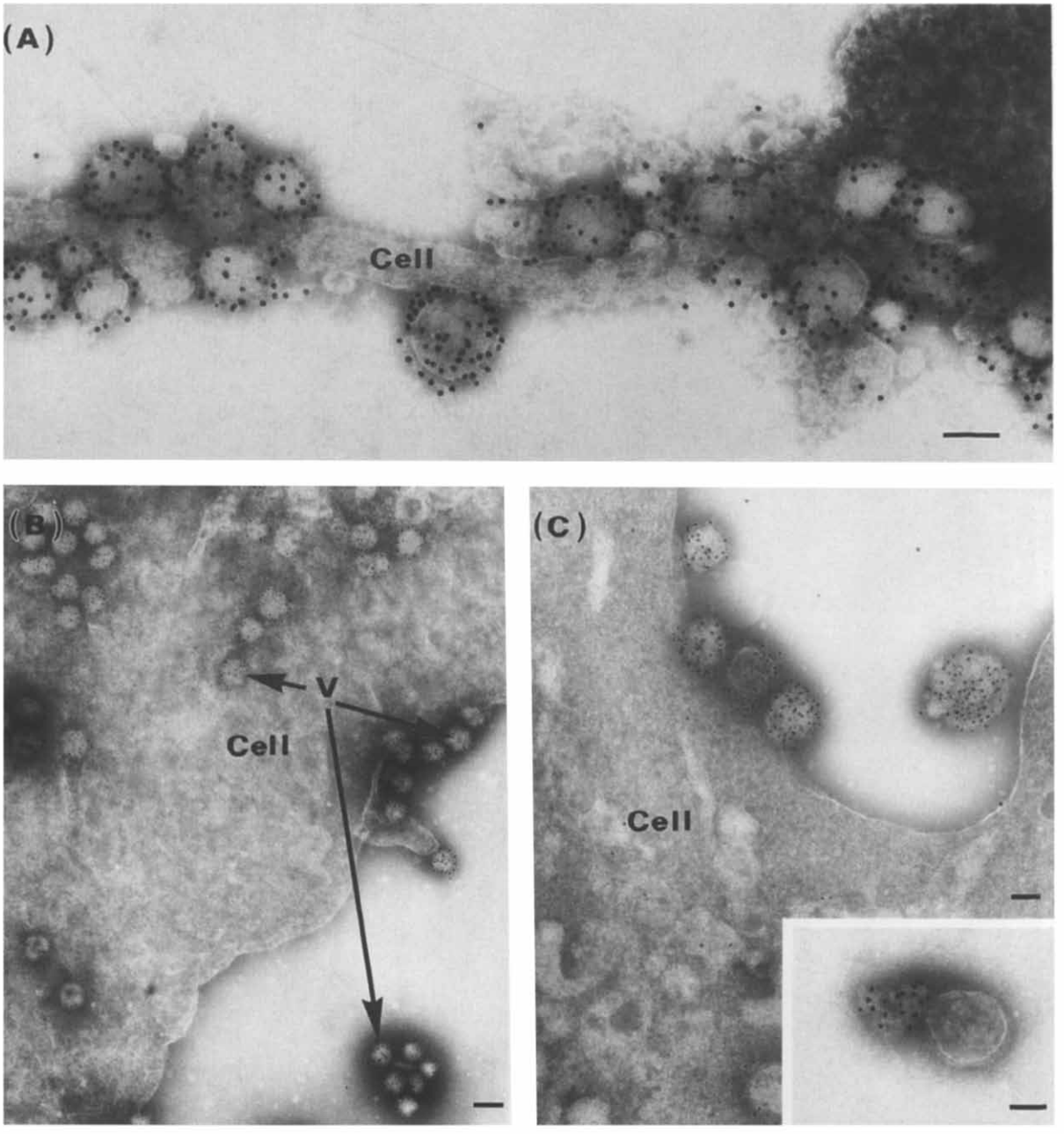

Fig. 13. Whole tissue culture cells, infected with different viruses and gold labelled 18–24 hr post-infection. (A) Herpesvirus (Aujesky's disease virus) detected with polyclonal antibodies and protein-A gold (12 nm). (B) Bunyavirus (Akabane) labelled with monoclonal antibody complexed to 12 nm colloidal gold. (C) Paramyxovirus (Newcastle disease virus) labelled with a 12 nm gold complexed monoclonal antibody to a surface protein and the nucleocapsid (inset). Viruses (V). Scales represent 100 nm.

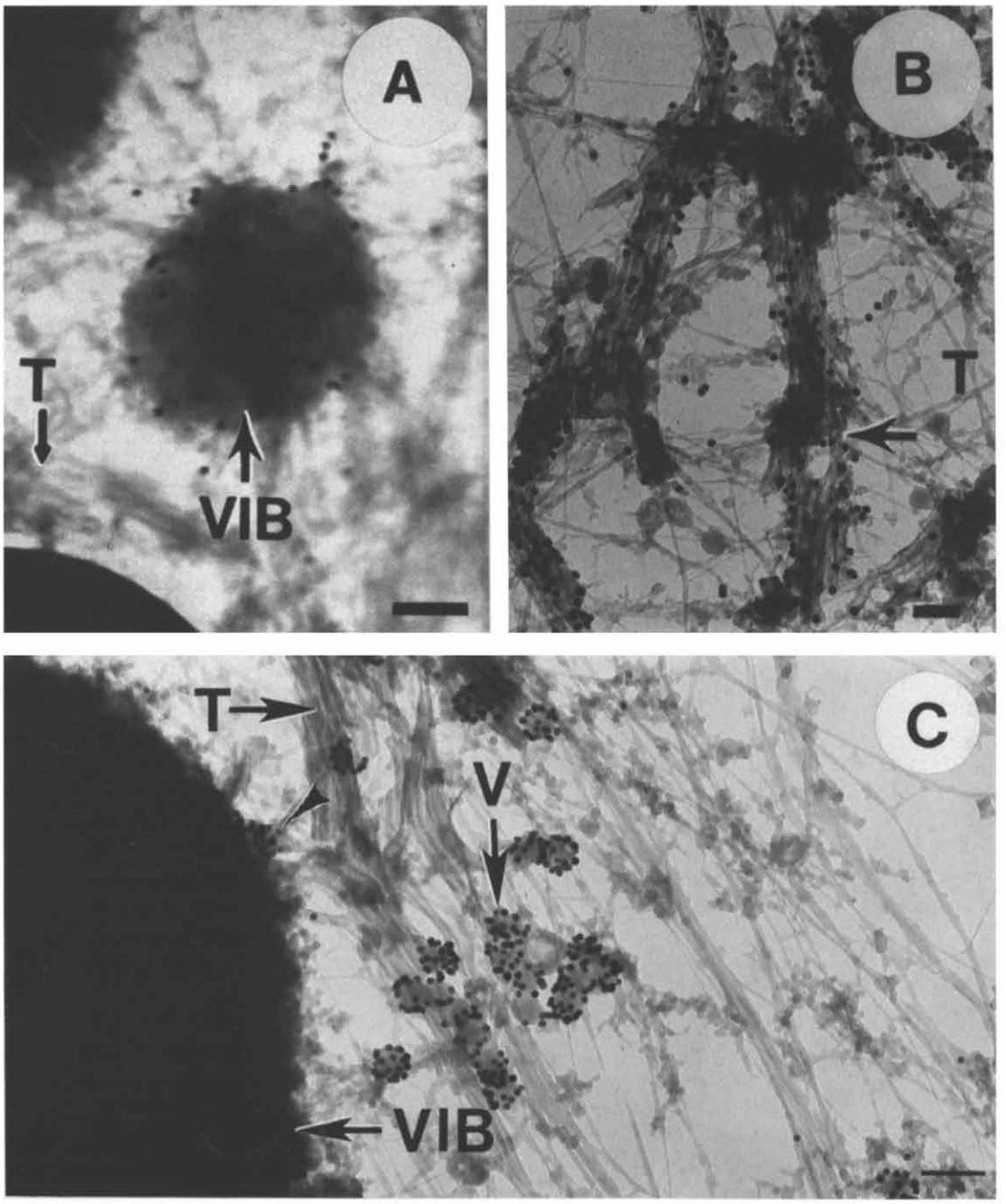

Fig. 14. Extracted bluetongue virus infected cells incubated with various monoclonal antibodies (Mab). (A) Scanning transmission electron micrograph (100 kV) of virus inclusion body (VIB) reacted with specific Mab (anti-NS2) and protein-A gold (12 nm). Tubules (T). (B) Virus tubules (T) reacted with specific Mab (anti-VP3) and protein-A gold; note similar result obtained when reacted with Mab to NS1 (refer Section VI.C). (C) Virus (V) reacted with gold complexed Mab (anti-VP2). Note close proximity of virus (arrow head) with virus inclusion body (VIB) (refer Section VI.C). Scales represent 100 nm. (Adapted from Eaton and Hyatt, 1989.)

antibody molecules will interact with their specific targets. Representative results obtained with IEM of extracted GCC are illustrated in Fig. 14. The labelling protocol is detailed by Hyatt *et al.* (1987).

Problems with immuno-gold labelling of cytoskeletal preparations can occur. The most common problem involves "sticky" gold probes, especially the smaller (6 nm) probes which may interact with the cytoskeletal matrix. This problem of non-specific binding is discussed in detail by Birrell *et al.* (1987) and Hyatt (1989) and is largely solved by substituting fish gelatin for the conventional bovine serum albumin stabilizer or by pre-adsorbing the antibody with non-infected cells.

The potential of the grid-cell-culture technique to preserve virus ultrastructure and to produce large numbers of adsorbed progeny viruses presents the virologist with an unique opportunity to undertake quantitative studies on comparative epitope density, efficacy of antibody binding and antibody competition (Eaton *et al.*, 1988; Gould *et al.*, 1988; Hyatt *et al.*, 1988). The studies can involve either single or double immuno-gold labelling. Figure 15 illustrates double-labelling of surface epitopes on a bunyavirus (Akabane) and an orbivirus (BTV). The results in Fig. 15C demonstrate that two neutralizing Mabs were directed to either the same or separate but neighbouring epitopes where the binding of one antibody inhibited the binding of the second (Hyatt *et al.*, 1988). Figure 15B demonstrates the "co-expression" of two BTV proteins namely VP2 and VP7 on the surface of the virus in an unstained critical point dried GCC preparation. The second example demonstrates the importance of virus structural preservation during preparative procedures as VP2 is a surface-associated protein easily removed during ultracentrifugation and VP7 is the major if not sole constituent of the underlying capsomers of the virus core particle. It should be noted that spurious results can be generated from double-labelling experiments unless various sources of error such as cross-contamination and degree of saturation of antigenic sites are determined. These sources of error are discussed by Hyatt *et al.* (1988) and Hyatt (1989).

B. *Scanning Electron Microscopy*

GCC can also be used for cell-surface studies involving topographic distribution of viruses during release and distribution of specific receptor sites. The examination of such preparations by standard SEM may be pertinent when the cells are too thick for the detection of gold-labelled surface-associated antigens by conventional TEM.

SEM can be used to detect colloidal gold probes by either secondary (SEI) or back-scattered electron imaging (BEI). The detection of smaller (5–15 nm) gold particles by SEI and standard instrumentation is difficult especially when the complex topography of the cell surface and the frequent presence of contaminating protein aggregates are taken into consideration. Detection of these smaller gold probes can be made with BEI in conjunction with higher resolution instruments (Hodges *et al.*, 1987). Alternatively larger probes (20–40 nm) can be used in conventional SEM and visualized independently or with a combination of BEI and SEI signals (Fig. 16A). Unfortunately the use of larger probes for the detection of virus specific antigens will sterically preclude a one-to-one correspondence of target to marker molecule and thus effectively decrease the overall labelling intensity. To avoid this problem 12 nm gold probes can be used and physically enhanced in size using the immuno-gold–silver staining (IGSS) technique (Hyatt *et al.*, 1989).

The IGSS protocol is similar to that described for GCC (Hyatt *et al.* 1987) except that a physical developing solution is included in the final steps (Hyatt *et al.*, 1989). The colloidal gold catalyzes the reduction of silver ions in the developing solution to metallic silver resulting in the physical growth of the electron-dense gold markers. The major advantages of this adaptation are that the silver enhanced probes are easily observed at low magnifications by a conventional scanning electron microscope utilizing SEI and/or BEI (Fig. 16B) and, as stated above, the avoidance of steric interference. Comparison between Figs 16A and 16B illustrate the increase in labelling obtained with the smaller probes. Details on post-fixation and coating procedures for these preparations are discussed by Hodges *et al.* (1987) and Hyatt *et al.* (1989).

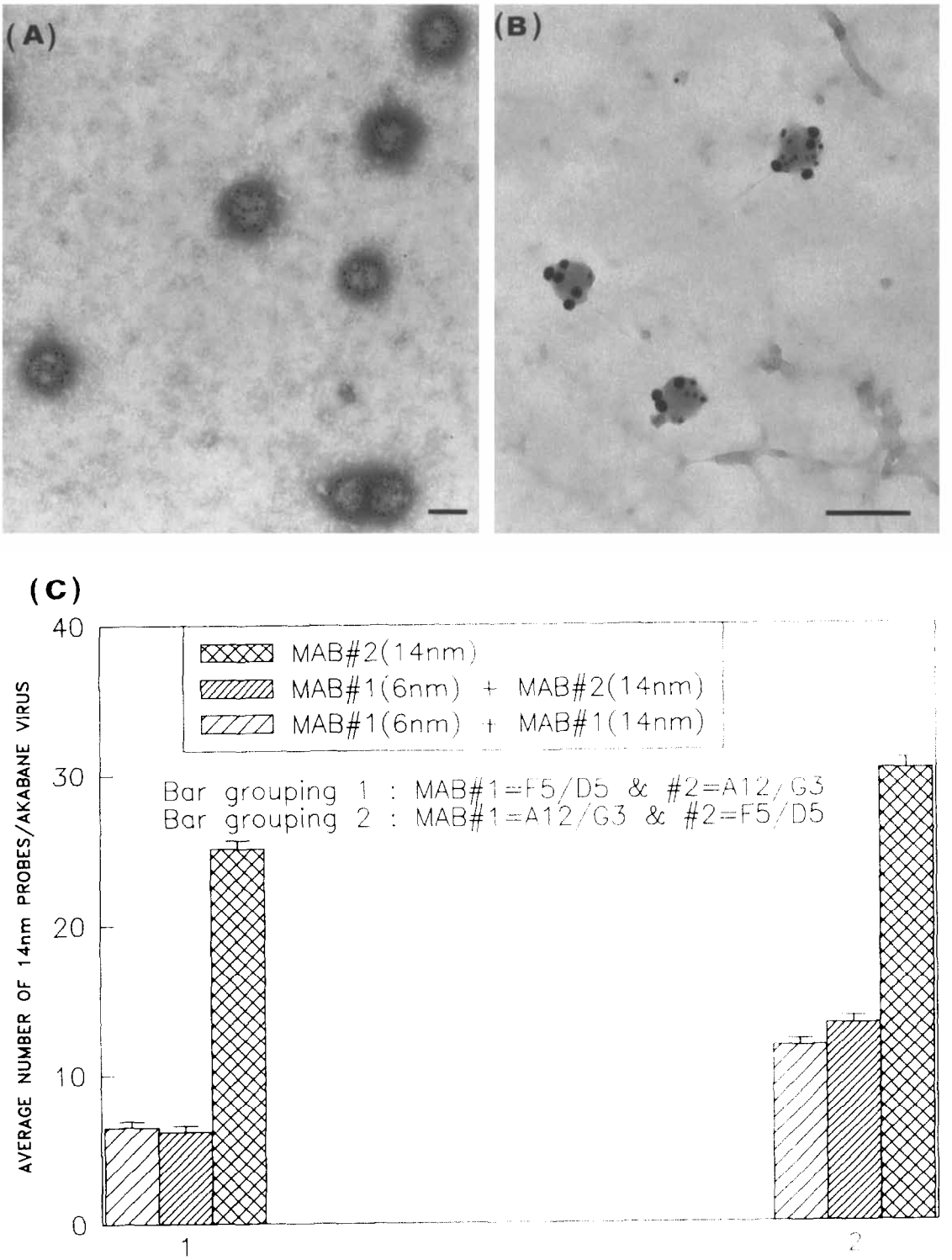

Fig. 15. Double labelling of viral surface epitopes. (A) Akabane virus labelled with different neutralizing monoclonal antibodies complexed to either 6 nm or 14 nm colloidal gold. (B) Double labelling of bluetongue virus (unstained) indicating the "co-expression" of two virus proteins VP2 and VP7. Note, similar results were obtained for virus proteins VP2 and NS1 (refer section VI.A). (C) Histograms showing the mean number of secondary 14 nm gold probes ± standard error for all immunological interactions. Scales represent 100 nm. (Adapted from Hyatt *et al.*, 1987.)

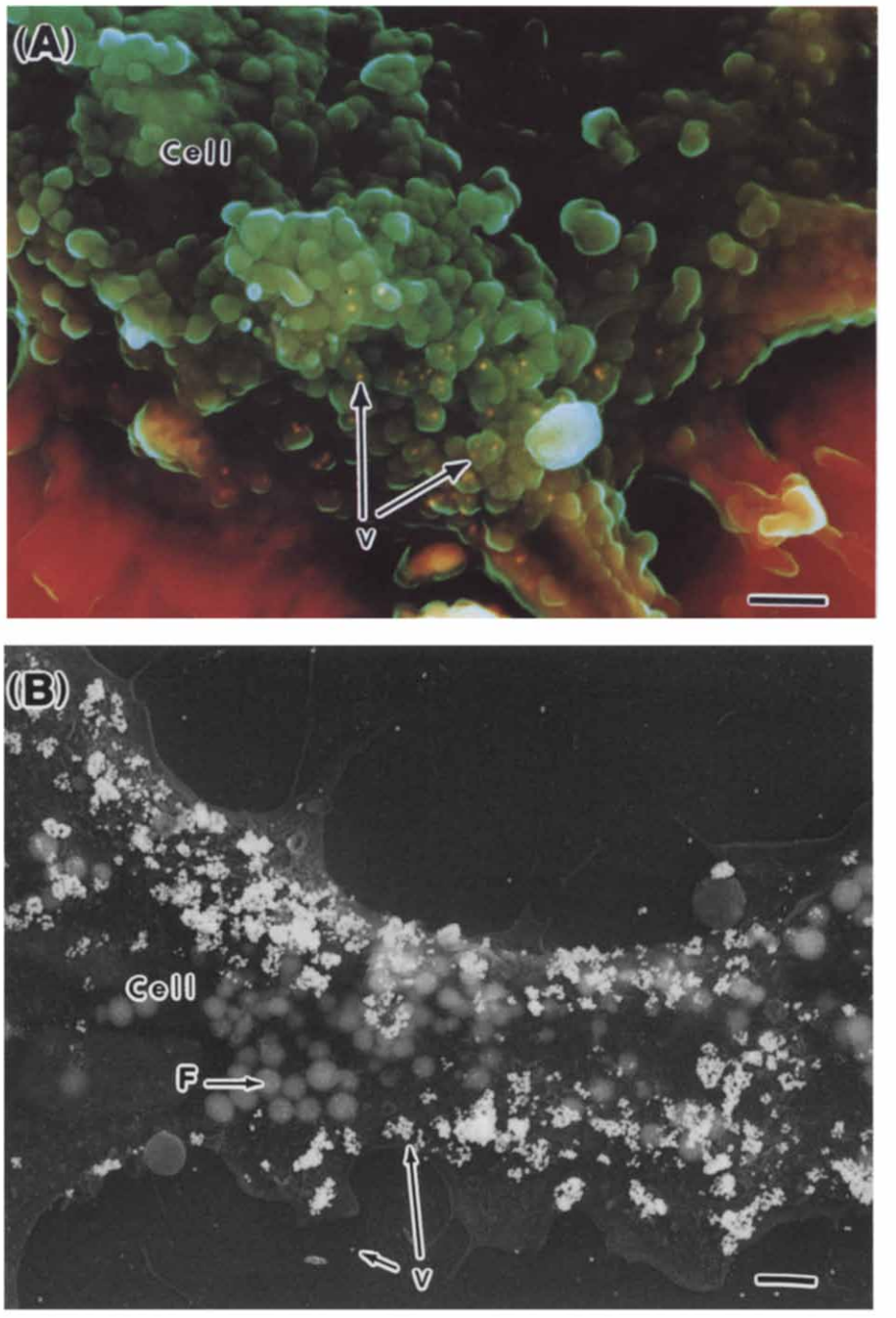

Fig. 16. Scanning electron micrographs of gold-labelled, bluetongue virus-infected grid-cell-cultures. (A) Colour electron micrograph of infected cells incubated with monoclonal antibody and 20 40 nm protein-A gold probes. The secondary electron image was recorded through a green filter and the inverted back-scattered image through a red filter onto colour positive film. Gold-labelled viruses (V). The cell was not post-fixed with osmium tetroxide and was coated with carbon. (B) Back-scattered image of a similar cell but labelled with 12 nm gold probes and silver enhanced for 6 min. The grid-cell-cultures were post-fixed in osmium tetroxide, thus the comparative strong signal from the osmophilic fat droplets (F) and were coated with chromium. Note the intensity of labelling between cells probed with 12 nm, and those with 20 40 nm protein-A gold probes. Scales represent 1 μm.

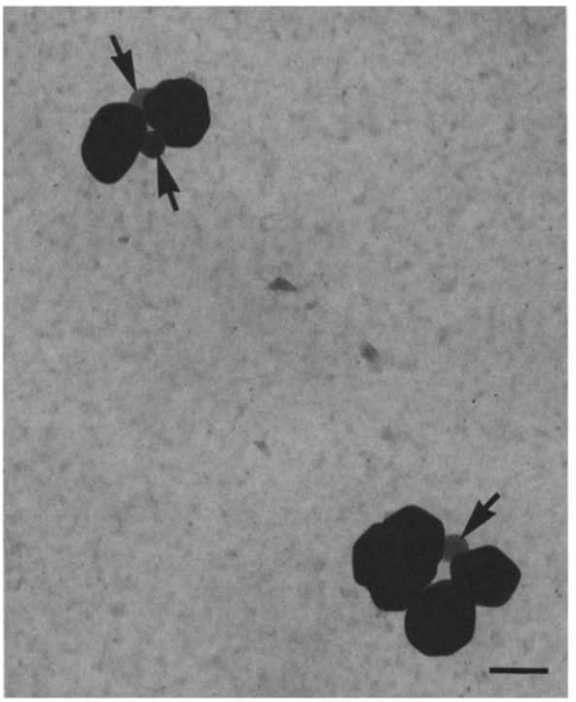

Fig. 17. Transmission electron micrograph of the bright "dots" localized on the grid substrate of gold silver labelled virus infected cells (refer Fig. 16B). Viruses (arrows) are not negatively stained. Scale represents 100 nm.

When GCC are used in the above manner, analogous preparations can be viewed by TEM (Fig. 17). For viral applications this will indicate the specificity of the "background" gold–silver labelling. For example, the particles present on the filmed substrate in Fig. 16B are gold–silver-labelled BTV and not the end product of indiscriminate background labelling.

VI. VIRUS STRUCTURE AND MORPHOGENESIS: BLUETONGUE VIRUS

The techniques described above can also be used in basic virological studies. In this section we shall describe how GCC have been used to investigate the surface-associated protein composition of BTV and related structures in addition to specific events in BTV morphogenesis. A detailed discussion of BTV morphogenesis is beyond the scope of this review but can be found in reviews by Eaton and Hyatt (1989) and Eaton *et al.* (1989).

A. *Virus Structure*

Morphologically BTV consists of an icosahedral core containing two major proteins, VP3 and VP7, and three minor proteins VP1, VP4 and VP6. The core is surrounded by an outer fibrillar coat consisting of two proteins, VP2 and VP5. The virus contains 10 segments of double-strandard RNA which code for the seven structural proteins and three non-structural proteins NS1, NS2 and NS3 (Verwoerd *et al.*, 1972; Huismans *et al.*, 1987; Eaton and Hyatt, 1989).

Until recently studies on the structure of BTV have used purified virus. As mentioned above (Section V. A) the biophysical and biochemical procedures employed during purification of virus particles such as BTV can lead to distortion or disruption and the removal of some proteins. It is therefore important, in any experiment involving the identification of virus substructure, to maintain the original structural composition and for this the grid-cell-culture technique is ideal.

We have used the technique to examine the surface "expression" of intrinsic virion proteins (Eaton *et al.*, 1988; Hyatt and Eaton, 1988). Viruses adsorbed to the grid substrate were probed with available Mabs to BTV proteins VP2, VP7, NS1 and VP3. Single and double-labelling experiments were attempted. The results showed the co-localization of VP2 with VP7 and VP2 with NS1 (Fig. 15). VP3 was not detected on the virion surface. These results in conjuction with conventional experiments utilizing purified BTV cores inferred that VP7 [known, from biochemical data, to be a major constituent of core capsomeres, Huismans *et al.* (1987)] and NS1 (previously thought to be solely an intracellular non-structural protein) extended beyond the core into the outer fibrillar coat where they were detected by specific Mabs.

B. *Intracellular and Extracellular Virus*

Extracted GCC were used to investigate the association of BTV with the cytoskeleton.

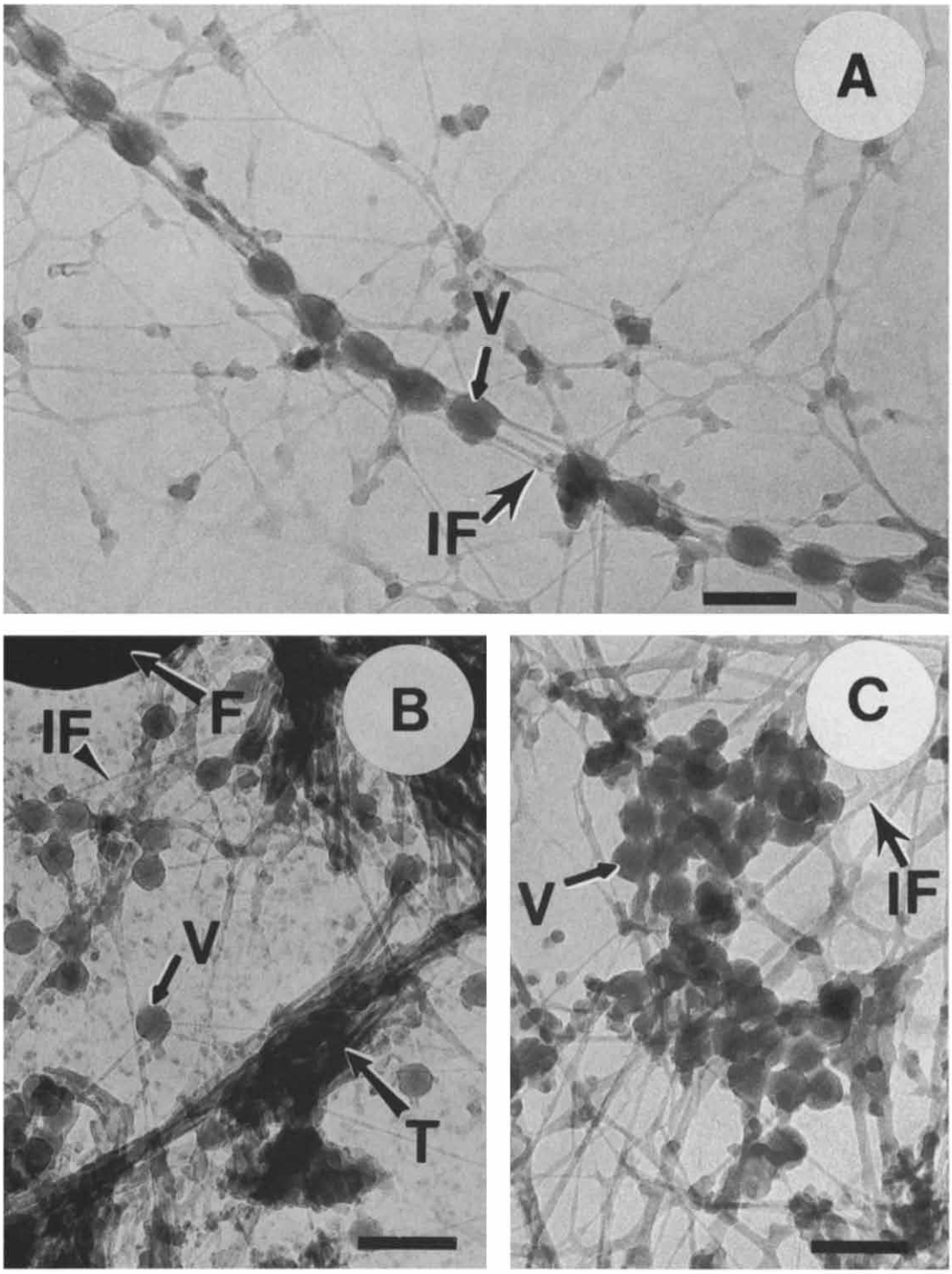

Fig. 18. Cytoskeleton-associated virus-like particles in bluetongue virus infected cells. (A) Linear array of viruses (V). Intermediate filaments (IF). (B) individual viruses (V) associated with the intermediate filaments (IF) of the cytoskeleton. Fat droplet (F); virus tubules (T). (C) Virus aggregate (V) associated with the cytoskeleton. Intermediate filaments (IF). Scales represent 100 nm. (Adapted from Eaton and Hyatt, 1989.)

Virus-like particles, identified by size and icosahedral shape, were located on the cytoskeleton either singularly, in linear arrays or in aggregates (Fig. 18). Evidence for the localization of viruses on intermediate filaments came from two experiments (Eaton *et al.*, 1987). The addition of cytochalasin B or colchicine, microfilament and microtubule disrupting drugs, respectively, did not result in the removal of virus-like particles from the cytoskeleton (Fig. 19A). In addition, filaments to which viruses were attached were labelled with colloidal gold-tagged anti-vimentin antibodies (Fig. 19B). The virus-like particles were confirmed to be BTV by the use of gold-labelled anti-VP2 antibody (Fig. 14C).

Previous work has shown that cytoskeletal-associated viruses exhibit a heterogeneous size range (64–74 nm) compared to released particles and those in the cytosol, i.e., cytoplasmic particles (64–67 nm) (Eaton *et al.*, 1989; Hyatt *et al.*, 1989). We have used a combination of extracted and non-extracted BTV-infected GCC and associated IEM techniques to investigate the properties of cytoskeletal-associated, cytoplasmic and released viruses. The experiments involved quantitative comparisons between the ability of the three populations to react with gold-labelled anti-VP2 Mab (Hyatt *et al.*, 1989). Released viruses, i.e., those adsorbed to the grid substrate outside the cell in unextracted preparations, were fixed with 0.1% glutaraldehyde and probed with a 12 nm gold-labelled anti-VP2 Mab. Other GCC were extracted and the cytoskeletal-associated viruses subsequently probed with the same gold-labelled antibody. The probing of cytoplasmic virus incorporated a double-labelling procedure

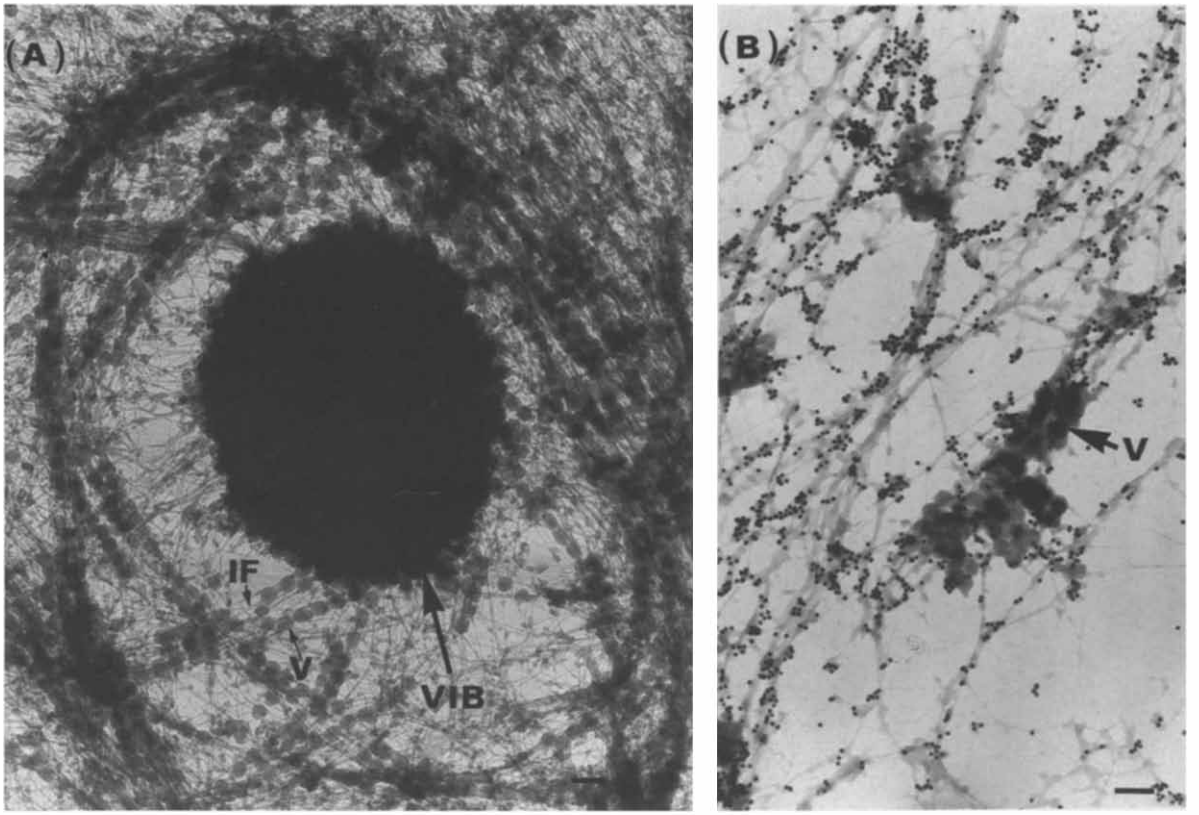

Fig. 19. (A) Redistribution of intermediate filaments (IF) around a virus inclusion body (VIB) of an extracted bluetongue virus (BTV) infected cell treated with colchicine (colchicine can induce re-organization of intermediate filaments, Eaton *et al.*, 1987). Note, the association of viruses with the intermediate filaments. (B) Intermediate filaments of an extracted BTV (V) infected cell labelled with gold anti-vimentin antibodies. Scales represent 100 nm. (Adapted from Eaton *et al.*, 1987.)

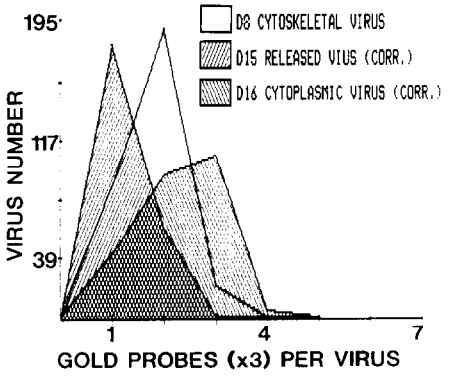

Fig. 20. Binding profiles of gold-labelled cytoskeletal bluetongue virus (BTV) (D8), released BTV (D15) and cytoplasmic BTV (D16). The gold labelling intensity for populations D15 and D16 have been corrected to allow for the effective inert surfaces, that is the virus surface area in contact with the grid substrate. (From Hyatt *et al.*, 1989.)

Released viruses were probed with a 6 nm gold-labelled anti-VP2 Mab, following which the cells were extracted and viruses probed with 12 nm gold-labelled antibody. Thus only viruses adsorbed to the grid substrate outside the cell and labelled solely with 12 nm gold probes have been released from the cytosol following cell lysis. The binding profiles (Fig. 20) indicate that there is a difference between the three populations in their ability to bind the antibody. Cytoplasmic virus bound most and released virus the least amount of gold-labelled antibody. These results infer that either VP2 is removed from intracellular virions during morphogenesis or alternatively the differences represent conformational changes in VP2 which obscure the reactive epitopes in some VP2 molecules.

C. *Location and Composition of Virus Specific Structures*

Electron microscopic examination of thin sections show that the cytoplasm of BTV-infected cells contains three major viral specific structures; viruses (discussed above), virus inclusion bodies (the site of virus core particle synthesis) and virus-specific tubules, the function of which is unknown. Cytoskeletons of BTV-infected GCC were characterized by the presence of dense areas in juxtanuclear positions. The majority of virus inclusion bodies and virus tubules were observed in these locations. Virus tubules were observed in bundles of upto 20 tubules and in advanced stages of infection were also localized in the peripheral areas of the cytoskeletal matrix. The virus inclusion bodies appeared to be penetrated by the complex anastomosing network of cytoskeletal filaments (Hyatt, unpublished observations) whereas the association of virus tubules with the cytoskeletal filaments remains unclear. Although the results indicated that these virus specific structures were associated with the cytoskeleton it is important to verify that the results are not a consequence of fortuitous adsorption incurred during the extraction procedure. Experiments utilizing virus inclusion body and virus tubule specific Mabs in conjunction with fluorescence were used to determine if these structures are found in the soluble fraction of the cell. Comparison of fluorescence patterns from both fixed, unextracted and extracted cells indicated that most if not all virus inclusion bodies are associated with the cytoskeleton whereas some virus tubules are present in the soluble phase. Such results support the findings from the extracted GCC studies.

Virus inclusion bodies and virus tubules located within extracted GCC are present as large antigenic masses when compared to those expressed in thin sections. Probing of virus tubules in extracted cells revealed a major core protein VP3 and the non-structural protein NS1 (Fig. 14B) to be present at a surface location. Similar probing experiments, using a biotin streptavidin system and lowicryl (K4M) failed to detect any associated protein; this is not surprising as the tubules are hollow and approximately 30 nm in diameter and thus in ultra-thin sections must present an extremely small antigenic mass. The advantage of using GCC in IEM is further exemplified by the probing of virus inclusion bodies. Post-embedding immunolabelling of ultra-thin lowicryl sections indicated the internal presence of core proteins VP7 and VP3 and the non-structural protein NS2 (Hyatt and Eaton, 1988). The presence of virus core proteins within virus inclusion bodies was consistent with a role for this structure in the morphogenesis of core particles. Labelling of extracted BTV-infected cells, however, indicated the presence of only NS2 on the surface of these inclusion

bodies (Fig. 14A). These results were confirmed with pre-embedding labelling experiments involving the examination of subsequently generated ultra-thin sections. Overall these approaches generated valuable data on the addition of viral proteins to developing particles (Gould *et al.* 1988; Eaton *et al.*, 1989).

One protein of particular interest in BTV morphogenesis is the outer coat protein VP2. This protein contains the major antigenic determinants responsible for serotype specificity and virus neutralization (Huismans and Erasmus, 1981). We were therefore interested in the site and mechanism of addition of this protein to the virus particle. VP2 was not located with the internal matrix of inclusion bodies (post-embedding procedures) or on the surface of this structure (GCC and pre-embedding procedures) (Gould *et al.*, 1988). The use of GCC and pre-embedding techniques however, indicated that Mab to VP2 reacted only in locations where virus-like particles appeared to be leaving the inclusion body (Figs 14C and 21). This example illustrates how the grid-cell-culture technique can be used as a powerful investigative tool when combined with other IEM techniques. It should also be noted that these examples illustrate the extreme care required in the overall interpretation of IEM results, particularly when they are generated by only one IEM approach.

D. *Mode of Virus Release*

The mechanism of BTV release from cells has been the subject of some speculation. The possibilities include virus release from dead or lysed cells, "budding" and release through "discontinuities" in the plasma membrane (Bowne and Jochim, 1967; Lecatsas, 1968; Bowne and Ritchie, 1970). When GCC were examined by TEM and SEM, 18–24 hr post-infection at which time 95% of the cells were still viable, large numbers of viruses were observed on the grid substrate and cell surface (Figs 12 and 16B). This simple experiment confirmed that virus release was not dependent upon

Fig. 21. Electron micrograph of a thin section from an extracted gold-labelled bluetongue virus infected cell. Gold-labelled viruses (arrows) can be seen at the periphery of a virus inclusion body (VIB). Compare with Fig. 14(C). Scale represents 100 nm. (Adapted from Gould *et al.*, 1988.)

cell death and subsequent lysis. The negative-stained GCC (Fig. 7C,D) showed individual BTV budding from the cell surface and aggregates in close proximity to disrupted areas of the host cell's plasma membrane. Examination of conventional and pre-embedded labelled ultra-thin sections also showed large virus aggregates partially embedded in the membrane. These results were interpreted as virus release as opposed to uptake (Eaton *et al.*, 1989; Hyatt *et al.*, 1989). The data suggest that (a) BTV was released both by "budding" and penetration of the plasma membrane by individual and aggregates of virus particles and (b) the different modes of release could occur in a single infected cell at the same time.

VII. CONCLUDING REMARKS

In the past, basic virological studies encompassing electron microscopy have largely depended on techniques involving virus purification, negative-staining and thin-sectioning. The same is true for virus diagnosis. In this review we have attempted to discuss the application of a technique using whole virus-infected cells to these areas of interest. The broad range of applications is attributed to several advantages inherent within the technique namely (a) rapid and simple preparative steps, (b) adsorption of large numbers of progeny viruses to the filmed grid substrate, (c) production of little or no contaminating debris and (d) preservation of virus and cellular morphology. Although the basic technique of growing virus-infected cells on filmed grids or equivalent substrates is not new, it is surprising that the full potential of this concept has not been fully appreciated, particularly in IEM where advanced quantitative studies can be easily performed. Another exciting area of use is in virus diagnosis. From the foregoing discussion and examples it is clear that the technique offers the potential for providing valuable additional diagnostic data, to that obtained by conventional procedures, within a short time period. Overall the technique, termed the grid-cell-culture technique, provides an attractive addendum to the more conventional techniques currently used in virus diagnosis and research.

Acknowledgements—We thank Terry Wise and Gary Crameri for their technical assistance and Mr. John White for supplying monoclonal antibodies.

REFERENCES

Adrian, M., Dubochet, J., Lepault, J. and McDowall, A. W., 1984. Cryo-electron microscopy of viruses. *Nature, Lond.*, **308,** 32–36.

Bauer, H. and Medzon, E. L., 1971. Freeze-etching technique for the study of virus ultrastructure. In: *Methods in Virology*. Vol. 5, Maramorosch, K. and Kaprowski, H. (eds), Academic Press, New York, 481–495.

Beesley, J. E., 1988. Bioapplication of colloidal gold in microbiological immunocytochemistry. *Scanning Microsc.*, **2,** 1055–1068.

Bell, P. B., 1981. The application of scanning electron microscopy to the study of the cytoskeleton of cells in culture. *Scanning Electron Microsc.*, Part 2, 139–157.

Bell, P. B., Lindroth, M. and Fredriksson, B. A., 1988. Preparation of cytoskeletons of cells in culture for high resolution scanning and scanning transmission electron microscopy. *Scanning Microsc.*, **2,** 1647–1661.

Ben-Ze'ev, A., Horowitz, M., Skolnik, H., Abulafia, R., Laub, O. and Aloni, Y., 1981. The metabolism of SV40 RNA is associated with the cytoskeletal framework. *Virology*, **111,** 475–487.

Ben-Ze'ev, A., Abulafia, R. and Aloni, Y., 1982. SV40 virions and viral RNA metabolism are associated with cellular substructures. *EMBO J.*, **1,** 1225–1231.

Ben-Ze'ev, A., Abulafia, R. and Bratosin, S., 1983. Herpes simplex virus and protein transport are associated with the cytoskeletal framework and the nuclear matrix in infected BSC-1 cells. *Virology*, **129,** 501–507.

Birdwell, C. R. and Strauss, J. H., 1974. Maturation of vesicular stomatitis virus: electron microscopy of surface replicas of infected cells. *Virology*, **59,** 587–590.

Birrell, G. B., Hedberg, K. K. and Griffith, O. H., 1987. Pitfalls of immunogold labeling: analysis by light microscopy, transmission electron microscopy, and photoelectron microscopy. *J. Histochem. Cytochem.*, **35,** 843–853.

Bohn, W., Rutter, G., Hohenberg, H., Mannweiler, K. and Nobis, P., 1986. Involvement of actin filaments in budding of measles virus: studies on cytoskeletons of infected cells. *Virology*, **149,** 91–106.

Borrelli, M. J., Koehm, S., Cain, C. A. and Tompkins, W. A. F., 1985. The effect of preparative protocol on the cytoskeleton ultrastructure observed in extracted whole-mount BHK cells. *J. Ultrastruct. Res.*, **91,** 57–65.

Bowne, J. G. and Jochim, M. M., 1967. Cytopathologic changes and development of inclusion bodies in cultured cells infected with bluetongue virus. *Am. J. vet. Res.*, **28,** 1091–1105.

Bowne, J. G. and Ritchie, A. E., 1970. Some morphological features of bluetongue virus. *Virology*, **40,** 903–911.

Brenner, S. and Horne, R. W., 1959. A negative staining method for high resolution electron microscopy of viruses. *Biochem. biophys. Acta*, **34,** 103–110.

Brown, S., Levinson, W. and Spudich, J. A., 1976. Cytoskeletal elements of chick embryos fibroblasts revealed by detergent extraction. *J. Supramolec. Struct.*, **5,** 119–130.

Buckley, I. K. and Porter, K. R., 1967. Cytoplasmic fibrils in living cultured cells. A light and electron microscopy study. *Protoplasma*, **64,** 349 380.

Buckley, I. K. and Porter, K. R., 1975. Electron microscopy of critical point dried whole cultured cells. *J. Microsc.*, **104,** 107 120.

Buckley, I. K. and Raju, T. R., 1976. Form and distribution of actin and myosin in non-muscle cells: a study using cultured chick embryo fibroblasts. *J. Microsc.*, **107,** 129 149.

Carrascosa, J. L., 1988. Immunoelectron microscopial studies on viruses. *Electron Microsc. Rev.*, **1,** 1 16.

Cervera, M., Dreyfuss, G. and Penman, S., 1981. Messenger RNA is translated when associated with the cytoskeletal framework in normal and VSV-infected HeLa cells. *Cell*, **23,** 113 120.

Choppin, P. W., 1963. On the emergence of influenza virus filaments from host cells. *Virology*, **21,** 278 281.

Dales, S., 1962. An electron microscope study of the early association between two mammalian viruses and their hosts. *J. Cell Biol.*, **13,** 303 322.

Darcy-Tripier, F., Nermut, M. V., Braunwald, J. and Williams, L. D., 1984. The organisation of frog virus 3 as revealed by freeze etching. *Virology*, **138,** 287 299.

De Harven, E., Beju, D., Evenson, D. P. and Basu, S., 1973. Structure of critical point dried oncornaviruses. *Virology*, **55,** 535 540.

Dubochet, J., Adrian, M., Lapault, J. and McDowall, A. W., 1985. Cryo-electron microscopy of vitrified biological specimens. *TIBS*, **10,** 143 146.

Eaton, B. T. and Hyatt, A. D., 1989. Association of bluetongue virus with the cytoskeleton. In: *Subcellular Biochemistry*, Vol 15, *Virally Infected Cells*, Harris, J. R. (ed.), Plenum, New York, 233 273.

Eaton, B. T., Hyatt, A. D. and White, J. R., 1987. Association of bluetongue virus with the cytoskeleton. *Virology*, **157,** 107 116.

Eaton, B. T., Hyatt, A. D. and White, J. R., 1988. Localization of the nonstructural protein NS1 in bluetongue virus-infected cells and its presence in virus particles. *Virology*, **163,** 527 537.

Eaton, B. T., Hyatt, A. D. and Brookes, S. M., 1989. The replication of bluetongue virus. *Curr. Top. Microbiol. Immunol.* (in press).

Grimly, P. M., 1970. High voltage electron microscope study of early stages in poxvirus morphogenesis. *J. Cell Biol.*, **47,** 79a.

Gould, A. R., Hyatt, A. D. and Eaton, B. T., 1988. Morphogenesis of a bluetongue virus variant with an amino acid alteration at a neutralization site in the outer coat protein, VP2. *Virology*, **165,** 23 32.

Hiller, G., Weber, K., Schneider, L., Parajsz, C. and Jungwirth, C., 1979. Interaction of assembled progeny pox viruses with the cellular cytoskeleton. *Virology*, **98,** 142 153.

Hodges, G. M., Southgate, J. and Toulson, E. C., 1987. Colloidal gold a powerful tool in scanning electron microscope immunocytochemistry: An overview of bio-applications. *Scanning Microsc.*, **1,** 301 318.

Hosaka, Y. and Watabe, T., 1988. Cryoelectron microscopy of vitrified Sendai virions. *J. Virol. Methods*, **22,** 347 349.

Huismans, H. and Erasmus, B. J., 1981. Indentification of the serotype-specific and group specific antigens of bluetongue virus. *Onderstepoort J. vet. Res.*, **48,** 51 58.

Huismans, H., Van Dijk, A. A. and Els, H. J., 1987. Uncoating of parental bluetongue virus to core and subcore particles in infected L cells. *Virology*, **157,** 180 188.

Hyatt, A. D., 1989. Protein-A gold: non specific binding and cross contamination. In: *Colloidal Gold*, Vol. 2, *Principles, Methods and Application*, Hayat, M. A. (ed.), Academic Press (in press).

Hyatt, A. D. and Eaton, B. T., 1988. Ultrastructural distribution of the major capsid proteins within bluetongue virus and infected cells. *J. gen. Virol.*, **69,** 805 815.

Hyatt, A. D., Eaton, B. T. and Lunt, R., 1987. The grid-cell-culture technique: the direct examination of virus-infected cells and progeny viruses. *J. Microscopy*, **145,** 97 106.

Hyatt, A. D., McPhee, D. A. and White, J. R., 1988. Antibody competition studies with gold-labelling immunoelectron microscopy. *J. Virol. Methods*, **19,** 23 32.

Hyatt, A. D., Eaton, B. T. and Brookes, S. M., 1989. The release of BTV from infected cells and their superinfection by progeny virus. *Virology* (in press).

Iwasaki, Y., 1978. Application of the critical point dried whole cell technique to the study of animal rhabdoviruses. *Intervirology*, **9,** 214 225.

Kilarski, W. and Koprowski, H., 1976. Observation of whole, cultured human brain cells using 100 kilovolts electron microscopy. *J. Microsc. Biol. Cell*, **25,** 73 80.

Kilarski, W., Iwasaki, Y., Porter, K. R. and Koprowski, H., 1976. High voltage electron microscopy of human brain cells infected with vaccinia and parainfluenza 1 viruses. *J. Microsc. Biol. Cell*, **25,** 81 86.

Kramarsky, B., Lasfargues, E. Y. and Moore, D. H., 1970. Ultrastructural and quantitative studies of mammary tumor virus production in cultured mouse mammary tumour cells. *Cancer Res.*, **30,** 1102 1108.

Lecatsas, G., 1968. Electron microscopic study of the formation of bluetongue virus. *Onderstepoort J. vet. Res.* **35,** 139 150.

Lenk, R. and Penman, S., 1979. The cytoskeletal framework and poliovirus metabolism. *Cell*, **16,** 298 301.

Lenk, R., Ransom, L., Kaufmann, Y. and Penman, S., 1977. A cytoskeletal structure with associated polyribosomes obtained from HeLa cells. *Cell*, **10,** 67 78.

Luftig, R. B. and Weihing, R. R., 1975. Adenovirus binds to rat brain microtubules *in vitro*. *J. Virol.*, **16,** 696 706.

Malech, H. L. and Wivel, N. A., 1976. Properties of murine intracisternal A particles. Electron microscopic appearance after critical point drying and platinum shadowing. *Virology*, **69,** 802 809.

Munz, E., Gobel, E. M. E., Krolopp, C., Reimann, M. and Davies, F. G., 1981. Electron microscopic studies on the morphology of Nairobi sheep disease virus. *Zentbl vet. Med. B*, **28,** 553 563.

Murphy, F. A., 1980. Togavirus morphology and morphogenesis. In: *The Togaviruses: Biology, Structure, Replication*, Schlesinger, R. W. (ed.), Academic Press, New York, 241 316.

Murphy, F. A., Harrison, A. K. and Whitfield, S. G., 1973. Bunyaviridae: Morphologic and morphogenetic similarities of Bunyamwera serologic supergroup viruses and several other arthropod-borne viruses. *Intervirology*, **1,** 297 316.

Murti, K. G., Porter, K. R., Goorha, R., Ulrich, M. and Wray, G., 1984. Interaction of frog virus 3 with the cytomatrix II. Structure and composition of the virus assembly site. *Expl Cell Res.*, **154,** 270 282.

Murti, K. G., Goorha, R. and Chen, M., 1985. Interaction of frog virus 3 with the cytoskeleton. *Curr. Top. Microbiol. Immunol.*, **116,** 107 131.

Nagai, Y., Yoshida, T., Hamaguchi, M., Nagura, H., Hasegawa, H., Yoshimura, S. and Watanabe, K., 1983. Subcellular location of the major protein antigens of paramyxoviruses revealed by immunoperoxidase cytochemistry. *Microbiol. Immunol.*, **27,** 531–545.

Nermut, M. V., 1972. Negative staining of viruses. *J. Microsc.*, **96,** 351–362.

Nermut, M. V., 1973. Freeze-drying and freeze-etching of viruses. In: *Freeze Etching, Techniques and Applications*, Benedetti. E. L. and Favard, P. (eds), Societe Francaise de Microscopie Electronique, Paris, 135–150.

Nermut, M. V., 1978. Structural elements in adenovirus cores. Studies by means of freeze-fracturing and ultrathin sectioning. *Arch. Virol.*, **57,** 323–337.

Nermut, M. V., 1982. Advanced methods in electron microscopy of viruses. In: *New Developments in Practical Virology*, Howard, C. R. (ed.), Alan R. Liss, New York, 1–58.

Ornelles, D. A., Fey, E. G. and Penman, S., 1986. Cytochalasin releases mRNA from the cytoskeletal framework and inhibits protein synthesis. *Mol. Cell Biol.*, **6,** 1650–1662.

Palmer. E. L. and Martin. M. L., 1982. Togaviridae. In: *An Atlas of Mammalian Viruses*, CRC Press, Boca Raton, Florida, 37–40.

Penman, S., 1985. Virus metabolism and cellular architecture. In: *Virology*, Fields, B. N. (ed.), Raven Press, New York, 169–182.

Sheffield, J. B., 1981. The use of freeze fracture, freeze etching and critical point drying for the study of enveloped viruses. *Micron*, **12,** 323–338.

Small, J. V., 1988. The actin cytoskeleton. *Electron Microsc. Rev.*, **1,** 155–174.

Stokes, G. V., 1976a. Vaccinia virus LS and NP-antibody labeling in whole infected African green monkey kidney BSC-1 cells studied by high voltage electron microscopy. *J. Cell Biol.*, **70,** 4a.

Stokes, G. V., 1976b. High-voltage electron microscope study of the release of vaccinia virus from whole cells. *J. Virol.*, **18,** 636–643.

Verwoerd, D. W., Els, H. J., De Villiers, E. M. and Huismans, H., 1972. Structure of the bluetongue virus capsid. *J. Virol.*, **10,** 783–794.

Vogel, R. H., Provencher, S. W., Von Bonsdorff, C. H., Adrian, M. and Dubochet, J., 1986. Envelope structure of Semliki Forest virus reconstructed from cryo-electron micrographs. *Nature, Lond.*, **320,** 533–535.

Von Bonsdorff, C. H. and Harrison, S. C., 1975. Sind bis virus glycoproteins form a regular icosahedral surface lattice. *J. Virol.*, **16,** 141–145.

Yoshida. M., Uno, F. and Nii, S., 1986. High voltage electron microscopy of whole cells infected with herpes simplex virus type 1. *J. Electron Microsc.*, **35,** 47–59.